European Journal of Taxonomy 930: 79–123
https://doi.org/10.5852/ejt.2024.930.2481

ISSN 2118-9773
www.europeanjournaloftaxonomy.eu
2024 · Stec D.

Research article

urn:lsid:zoobank.org:pub:A09EB44B-286F-439A-A970-48F09416584A

Integrative taxonomy supports two new species of *Macrobiotus* (Tardigrada: Eutardigrada: Macrobiotidae) allowing further discussion on the genus phylogeny

Daniel STEC

Institute of Systematics and Evolution of Animals, Polish Academy of Sciences, Sławkowska 17, 31-016 Kraków, Poland.

E-mail: daniel.stec@isez.pan.krakow.pl, daniel_stec@interia.eu

urn:lsid:zoobank.org:author:13C435F8-25AB-47DE-B5BB-8CE788E92CF6

Abstract. In this study, I describe two new species of *Macrobiotus* based on morphological data collected through light and scanning electron microscopy. Both species are accompanied by DNA sequences from four commonly used molecular markers (18S rDNA, 28S rDNA, ITS-2, and COI). *Macrobiotus ovovittatus* sp. nov. was discovered in Greenland and can be distinguished from similar taxa of *Macrobiotus* by its continuous, solid, and clearly wrinkled egg surface, adorned with sparse, very small and irregularly spaced pores. Additionally, the terminal discs of egg processes are covered in multiple light-refracting dots, resembling crocheted napkins. *Macrobiotus mileri* sp. nov. was found in Israel and is characterized by unique pore arrangements in its body cuticle, expressed in two distinct animal forms: (i) forma porata with large pores arranged in five distinct patches and (ii) forma aporata with single, almost undetectable pores. It also features weakly defined convex terminal discs with smooth edges. Furthermore, the phylogenetic analyses conducted in this study offer the most updated phylogeny of superclade I within the family Macrobiotidae. This facilitates additional discussion concerning the interrelationships among species within the genus *Macrobiotus* and the circumscription of species groups within it.

Keywords. Egg ornamentation, morphology, *Macrobiotus polonicus-persimilis* species complex, new species, water bears.

Stec D. 2024. Integrative taxonomy supports two new species of *Macrobiotus* (Tardigrada: Eutardigrada: Macrobiotidae) allowing further discussion on the genus phylogeny. *European Journal of Taxonomy* 930: 79–123. https://doi.org/10.5852/ejt.2024.930.2481

Introduction

Tardigrades are a phylum of small invertebrates, with a body size rarely exceeding 1 mm. They are considered part of the meiofauna because they require at least a thin film of water surrounding their bodies to carry out all life activities. Currently, nearly 1500 recognized species have been discovered

worldwide in various habitats. However, the majority of these species have been found in limno-terrestrial environments, inhabiting mosses and lichens. (Nelson *et al.* 2019; Degma & Guidetti 2023).

One of the most speciose and diverse limno-terrestrial cosmopolitan tardigrade groups is the family Macrobiotidae, which comprises approximately 340 nominal species and subspecies classified within 14 genera (Stec *et al.* 2021a; Degma & Guidetti 2023). Importantly, among them, the genus *Macrobiotus* Schultze, 1834 seems to have the most complicated revisional history. This tardigrade group exhibits extreme phenotypic diversity, particularly in terms of egg ornamentation morphologies (Guidetti *et al.* 2013; Kaczmarek & Michalczyk 2017; Stec *et al.* 2021a; Kaczmarek *et al.* 2023). Therefore, it is not surprising that several recent studies have sparked lively discussions and efforts to obtain a more uniform definition for the genus, as well as smaller species groups within it (Kaczmarek & Michalczyk 2017; Massa *et al.* 2021; Stec *et al.* 2021a, 2021b, 2022; Vecchi & Stec 2021; Kaczmarek *et al.* 2023; Bertolani *et al.* 2023). Nevertheless, due to the exceptionally vast morphological diversity that cannot be easily accommodated within clear and strict man-made definitions while also considering phylogenetic relationships, a satisfactory consensus has not yet been reached. For now, only the fact of the internal division of *Macrobiotus* into three distinct and deeply divergent phylogenetic lineages has been well supported by several studies (clades A, B, and C, respectively; Stec *et al.* 2021a, 2022; Vecchi & Stec 2021; Bertolani *et al.* 2023). Several smaller groups (morphologically uniform) within the genus have also been supported as monophyletic, and as such, they were confirmed as species complexes: *M. pallarii* complex (Stec *et al.* 2021a, 2021b), *M. pseudohufelandi* complex (Stec *et al.* 2021a), *M. ariekammensis* complex (Stec *et al.* 2022), and *M. polonicus* complex (Stec *et al.* 2021a; Vecchi & Stec 2021). The latter was recently reinvestigated and redefined as the *M. polonicus-persimilis* complex by Bertolani *et al.* (2023). All remaining taxa of *Macrobiotus* have been accommodated into informal species morpho-groups that are not monophyletic: *M. hufelandi* morpho-group (Stec *et al.* 2021a), *M. nelsonae* complex (Stec *et al.* 2021a; redefined into morpho-group by Kaczmarek *et al.* 2023), and *M. persimilis* morpho-group (Bertolani *et al.* 2023). These grouping strategies allowed all taxa of *Macrobiotus* to be assigned to one of these groups, especially thanks to the very general definition of the *M. hufelandi* morpho-group, which now serves also as a basket for undecided species. However, these subdivisions might have been considered still too complicated or not sufficient for taxonomists and other name users. Therefore, Kaczmarek *et al.* (2023) proposed a solution that neglects phylogenetic relationships, providing an artificial division of all taxa of *Macrobiotus* into 12 morphological groups based on eggshell morphology. Theoretically, such action might be helpful in facilitating taxonomic or faunistic research and better navigation between taxa within the tardigrade group, but time will show if the community will acknowledge and utilize this approach.

In this paper, I propose integrative descriptions of two new species of *Macrobiotus*. For both of them, I provide detailed morphological and morphometric data obtained through light and scanning electron microscopy, along with a set of DNA sequences from the four molecular markers commonly used in tardigrade taxonomy. Additionally, I present an updated molecular phylogeny of superclade I of the family Macrobiotidae, which includes the genera *Macrobiotus*, *Mesobiotus* Vecchi, Cesari, Bertolani, Jönsson, Rebecchi & Guidetti, 2016, and *Sisubiotus* Stec, Vecchi, Calhim & Michalczyk, 2021. These results allow for a discussion of the phylogeny of the genus *Macrobiotus* and the species composition of the groups distinguished within it.

Material and methods

Sample processing

A moss sample (GL.001) containing one new species was collected in Greenland near Zackenberg Valley by Michał Kolasa in July 2021. Another moss sample (IL.001), containing a second new species, was collected in Tel-Aviv, Israel, by Krzysztof Miler in November 2019. Samples were examined for

terrestrial tardigrades using standard methods as described in Stec *et al.* (2015). In order to perform integrative taxonomic descriptions, isolated animals and eggs extracted from both samples were split into three groups for specific analyses: morphological analysis with phase contrast light microscopy, morphological analysis with scanning electron microscopy, and DNA sequencing (for details please see sections "Material examined" provided below for each species description). Additionally, 10 females with oocytes on different developmental stages and 5 smaller animals without visible oocytes from the sample GL.001 were stained with aceto-orcein staining to check the presence of sperm (Bertolani 1971).

Microscopy and imaging

Specimens for light microscopy were mounted on microscope slides in a small drop of Hoyer's medium and secured with a cover slip, following the protocol by Morek *et al.* (2016). Slides were then dried for five to seven days at 60°C. Dried slides were sealed with a transparent nail polish and examined under a Leica DMLB light microscope with phase contrast (PCM), associated with an digital camera (DLT-Cam PRO). Immediately after mounting the specimens in the medium, slides were also checked under PCM for the presence of males and females in the studied population, as the spermatozoa in testis and vas deferens are visible only for several hours after mounting (Coughlan *et al.* 2019; Coughlan & Stec 2019). In order to obtain well-extended animals and clean eggs for SEM, the specimens were processed according to the protocol by Stec *et al.* (2015). In short, eggs were first subjected to a water/ethanol and an ethanol/acetone series, then to CO_2 critical point drying and finally sputter coated with a thin layer of gold. Specimens were examined under high vacuum in a Versa 3D Dual Beam Scanning Electron Microscope at the ATOMIN facility of the Jagiellonian University, Kraków, Poland. All figures were assembled in Corel Photo-Paint X6. For structures that could not be satisfactorily focused in a single photograph, a stack of 2–6 images was taken with an equidistance of ca 0.2 µm and assembled manually into a single deep-focus image.

Morphometrics and morphological nomenclature

All measurements are given in micrometres (µm). Sample size was adjusted following recommendations by Stec *et al.* (2016a). Structures were measured only if their orientation was suitable. Body length was measured from the anterior extremity to the end of the body, excluding the hind legs. The buccal apparatus and claws were classified according to Pilato & Binda (2010). The terminology used to describe oral cavity armature and egg shell morphology follows Kaczmarek & Michalczyk (2017). Macroplacoid length sequence is given according to Kaczmarek *et al.* (2014) whereas morphological states of cuticular bars on legs follow Kiosya *et al.* (2021). Buccal tube length and the level of the stylet support insertion point were measured according to Pilato (1981). The pt index is the ratio of the length of a given structure to the length of the buccal tube expressed as a percentage (Pilato 1981). All other measurements and nomenclature follow Kaczmarek & Michalczyk (2017). Buccal tube width was measured as the external and internal diameter at the level of the stylet support insertion point. Lengths of the claw branches were measured from the base of the claw (i.e., excluding the lunula) to the top of the branch, including accessory points. Distance between egg processes was measured as the shortest distance between the base edges of the two closest processes. Morphometric data were handled using the "Parachela" ver. 1.8 template available from the Tardigrada Register (Michalczyk & Kaczmarek 2013) and are given in Supplementary files (Supp. file 1, Supp. file 2). Tardigrade taxonomy follows Bertolani *et al.* (2014) and Stec *et al.* (2021a).

DNA sequencing

The DNA was extracted from individual animals following a Chelex® 100 resin (Bio-Rad) extraction method by Casquet *et al.* (2012) with modifications described in detail in Stec *et al.* (2020a). Before the DNA extraction, each specimen was mounted on slides with water and checked under a light microscope. Four DNA fragments differing in mutation rates were sequenced. Namely: the small ribosome subunit

Table 1. Primers with their original references used for amplification of the four DNA fragments sequenced in the study.

DNA marker	Primer name	Primer direction	Primer sequence (5'-3')	Primer source
18S rRNA	18S_Tar_Ff1	forward	AGGCGAAACCGCGAATGGCTC	Stec *et al.* (2017a)
	18S_Tar_Rr1	reverse	GCCGCAGGCTCCACTCCTGG	
28S rRNA	28SF0002	forward	GRCRAGAKTACCCGCTGAAC	Mironov *et al.* (2012); Stec (2022a)
	28SR0990	reverse	CCTTGGTCCGTGTTTCAAGAC	
ITS-2	ITS2_Eutar_Ff	forward	CGTAACGTGAATTGCAGGAC	Stec *et al.* (2018a)
	ITS2_Eutar_Rr	reverse	TCCTCCGCTTATTGATATGC	
COI	LCO1490-JJ	forward	CHACWAAYCATAAAGATATYGG	Astrin & Stüben (2008)
	HCO2198-JJ	reverse	AWACTTCVGGRTGVCCAAARAATCA	

(18S rRNA, nDNA), the large ribosome subunit (28S rRNA, nDNA), the internal transcribed spacer (ITS-2, nDNA), and the cytochrome oxidase subunit I (COI, mtDNA). All fragments were amplified and sequenced according to the protocols described in Stec *et al.* (2020a); primers are listed in Table 1. Sequencing products were read with the ABI 3130xl sequencer at the Genomed company (Warsaw, Poland). Sequences were processed in BioEdit ver. 7.2.5 (Hall 1999) and submitted to GenBank. Prior submission all obtained COI sequences were translated into protein sequences in MEGA11 (Tamura *et al.* 2021) to check against pseudogenes.

Phylogenetic analysis and molecular species delimitation

To establish phyletic positions of both new species, a phylogenetic tree was constructed. For this purpose, a data set was compiled from taxa for which DNA sequences of at least two (out of all four analyzed in this study) molecular sequences are available and suitable for concatenation (Appendix 1). The only exception were sequences of *M.* cf. *nelsonae* from Bertolani *et al.* (2014) and *Macrobiotus muralis* Bertolani, Cesari, Giovannini, Rebecchi, Guidetti, Kaczmarek & Pilato, 2022 from Bertolani *et al.* (2023) for which only 18S rDNA sequences are currently available. DNA sequences of three species that represents Macrobiotidae super clade II sensu Stec *et al.* (2021a) where used as outgroup (Appendix 1). The sequences were aligned using the AUTO method (for COI and ITS-2) and the Q-INS-I method (for ribosomal markers: 18S rRNA and 28S rRNA) of MAFFT ver. 7 (Katoh *et al.* 2002; Katoh & Toh 2008) and manually checked against non-conservative alignments in BioEdit. The aligned sequences were trimmed to: 1064 (18S rRNA), 858 (28S rRNA), 658 (COI) bp. The ITS-2 alignment was processed using GBlocks ver. 0.91b (Castresana 2000; https://www.biologiaevolutiva.org/jcastresana/Gblocks.html) to remove ambiguously aligned regions, using the default 'less stringent' settings, and its final length was 236 bp. The sequences were then concatenated using SequenceMatrix (Vaidya *et al.* 2011). Before partitioning, the concatenated alignment was divided into 6 data blocks constituting three separate blocks of ribosomal markers and three separate blocks of three codon positions in the COI data set. Using PartitionFinder (Lanfear *et al.* 2016) under the Akaike Information Criterion (AIC), the best scheme of partitioning and substitution models was chosen for a Bayesian phylogenetic analysis. Bayesian inference (BI) marginal posterior probabilities were calculated for the concatenated (18S rRNA+28S rRNA+ITS-2+COI) data set using MrBayes ver. 3.2 (Ronquist & Huelsenbeck 2003). Random starting trees were used and the analysis was run for fifteen million generations, sampling the Markov chain every 1000 generations. An average standard deviation of split frequencies of < 0.01 was used as a guide to ensure the two independent analyses had converged. The program Tracer ver. 1.6 (Rambaut *et al.* 2014) was then used to ensure Markov chains had reached stationarity, and to determine the correct 'burn-in' for the analysis which was the first 10% of generations. The ESS values were greater than 200 and the consensus tree was obtained after summarising the resulting topologies and discarding the 'burn-in'. ModelFinder (Kalyaanamoorthy *et al.* 2017) was used to choose the best-fit models according

to the AIC for Maximum Likelihood (ML) analysis. Then, a ML reconstruction was conducted using W-IQ-TREE (Nguyen *et al.* 2015; Trifinopoulos *et al.* 2016). One thousand ultrafast bootstrap (UFBoot) replicates were applied to provide support values for branches (Hoang *et al.* 2018). The consensus trees was viewed and visualized by FigTree ver. 1.4.3 available from http://tree.bio.ed.ac.uk/software/figtree. The best evolutionary models of sequence evolution selected for BI and ML analyses, as well as respective raw trees, are given in Supplementary files (Supp. file 3). Additionally, the COI data set was used for genetic species delimitation with ASAP analysis, after removing the outgroups. Two analyses have been conducted: (i) one for the whole COI data set representing Mcrobiotidae super clade I and (ii) the second one for taxa of *Macrobiotus* only. Both analyses were run on the respective server (https://bioinfo.mnhn.fr/abi/public/asap/asapweb.html) with default settings. The outputs from the ASAP analyses are given in Supp. file 4.

Abbreviations

ISEA PAS = Institute of Systematics and Evolution of Animals, Polish Academy of Sciences, Sławkowska 17, 31-016 Kraków, Poland

PCM = phase contrast light microscopy
pt = index showing ratio of the length of a given structure to the length of the buccal tube, expressed as a percentage
SEM = scanning electron microscopy

Results

Taxonomic treatment

Phylum Tardigrada Doyère, 1840
Class Eutardigrada Richters, 1926
Order Parachela Schuster, Nelson, Grigarick & Christenberry, 1980
Superfamily Macrobiotoidea Thulin, 1928 (in Marley *et al.* 2011)
Family Macrobiotidae Thulin, 1928
Genus ***Macrobiotus*** Schultze, 1834

Macrobiotus ovovittatus sp. nov.
urn:lsid:zoobank.org:act:9C2931D3-8EBE-47AB-A3B0-991AB28F03A2
Figs 1–8, Tables 2–3

Etymology

The species name refers to the terminal discs of the egg processes which resemble crocheted napkins. From the Latin “egg” = “ovo” and “chaplet” = “vittatus”.

Material examined

32 animals, 57 eggs mounted on microscope slides in Hoyer’s medium, 15 animals and 15 eggs examined under SEM, 15 animals stained with orcein and two animals processed for DNA sequencing.

Type material

Holotype

GREENLAND • near Zackenberg Valley; 74°29′0.766″ N, 20°32′18.308″ W; 77 m a.s.l.; Jul. 2021; M. Kolasa leg.; mixed sample of moss and lichen collected from the rock in arctic tundra; ISEA PAS, slide GL.001.01.

Paratypes

GREENLAND • 46 animals; same collection data as for the holotype; ISEA PAS, slides GL.001.01 to GL.001.03, SEM stub TAR.015 • 72 eggs; same collection data as for the holotype; ISEA PAS, slides GL.001.04 to GL.001.09, SEM stub TAR.015.

Description

Animals

Body transparent in juveniles and white in adults, after fixation in Hoyer's medium transparent (Fig. 1A). Eyes present. Round and oval pores (0.4–0.6 μm in diameter), scattered randomly throughout the cuticle (distributed more sparsely on the ventral side of the body) (Figs 1B–E, 2A–B), including the external and internal surface of all legs (Fig. 3A–F). Granulation is present on the entire body cuticle and clearly visible under PCM and SEM, with granulation on the ventral side of the body being less dense (Figs 1B–E, 2A–B). Moreover, evident dense granulation patches on the external and internal surface of all legs I–III are visible under PCM and SEM (Fig. 3A–D). This dense granulation is also present on the lateral and dorsal surfaces of legs IV (Fig. 3E–F). A pulvinus-shaped cuticular bulge is centrally present on the internal surface of all legs I–III (Fig. 3C–D). This structure is visible only if the legs are fully extended and well oriented.

Claws small and slender, of the *hufelandi* type (Fig. 4A–F). Primary branches with distinct accessory points, a long common tract, and an evident stalk connecting the claw to the lunula (Fig. 4A–F). The lunulae on legs I–III are smooth (Figs 4A, D, E), while there is a dentation in the lunulae on legs IV (Fig. 4B, C, F). A single continuous cuticular bar and double muscle attachments are present above claws I–III (Figs 3C–D, 4A, D, E). Shadowed extensions that extend from the lunulae of the claws on legs I–III are present and visible only under PCM (Figs 3C, 4A). A horseshoe-shaped structure connects the anterior and posterior lunules on leg IV (Fig. 4B).

Mouth antero-ventral. Bucco-pharyngeal apparatus of *Macrobiotus* type, with ventral lamina and ten small peribuccal lamellae followed by six buccal sensory lobes (Figs 5A, 6A–B). Under PCM, the oral cavity armature is of *hufelandi* type – three bands of teeth are always visible (Fig. 5B–C). The first band of teeth is composed of numerous extremely small cones arranged in four to six rows located anteriorly in the oral cavity, at the bases of the peribuccal lamellae and just behind them (Figs 5B–C, 6A–B). The second band of teeth is located between the ring fold and the third band of teeth and comprises 4–6 rows of small cones, larger than those of the first band (Figs 5B–C, 6A–B). The teeth of the third band are located within the posterior portion of the oral cavity, between the second band of teeth and the opening of the buccal tube (Figs 5B–C, 6A–B). The third band of teeth is discontinuous and divided into the dorsal and ventral portions. Under PCM, the dorsal teeth are seen as three distinct transverse ridges, whereas the ventral teeth appear as two separate lateral transverse ridges between which a round median tooth is visible (Fig. 5B–C). Under SEM, both dorsal and ventral teeth are also clearly distinct (Fig. 6A–B). Under SEM, the margins of the dorsal teeth are clearly serrated (Fig. 6A) whereas the margins of the ventral teeth are less serrated (Fig. 6B). Pharyngeal bulb spherical, with triangular apophyses, two rod-shaped macroplacoids and a large triangular microplacoid (Fig. 5A). The macroplacoid length sequence being 2 < 1. The first and the second macroplacoid are constricted centrally and subterminally, respectively (Fig. 5D–E). The animals' measurements and statistics are given in Table 2.

Eggs

Laid freely, white, spherical and ornamented (Figs 7A–H, 8A–F). The surface between processes is of intermediate state between the *maculatus* and the *persimilis* type, that is, the surface is continuous/solid and clearly wrinkled with sparse, very small and irregularly spaced pores (Figs 7B, D, F, 8C–D). These pores are faintly visible under PCM but clearly visible under SEM (0.3–0.5 μm in diameter; Figs 7B, D, F, 8C–D). Under PCM the wrinkles in egg surface are visible as dark dots/comas/bars making the

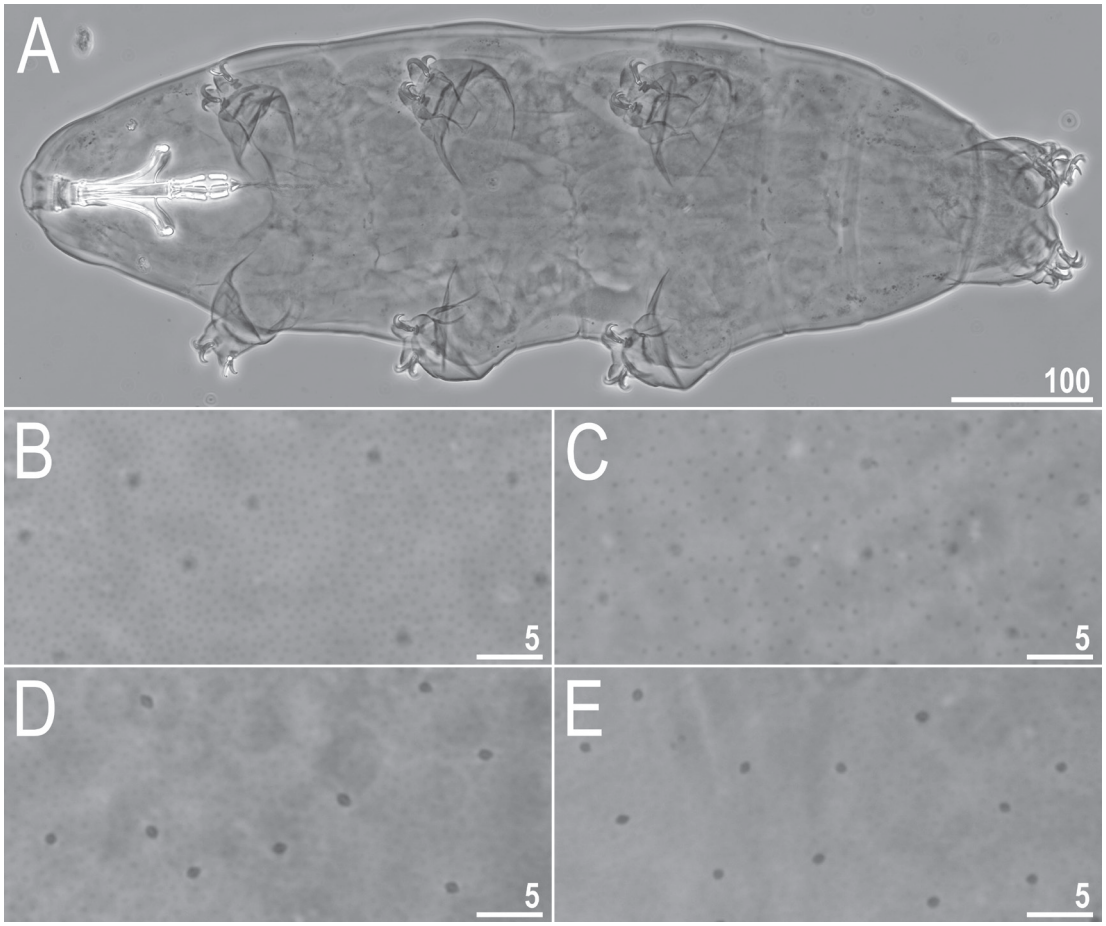

Fig. 1. *Macrobiotus ovovittatus* sp. nov., PCM images of habitus, body granulation and cuticular pores of the holotype (GL.001.01, ISEA PAS). **A**. Habitus, dorso-ventral projection. **B**. Granulation in the dorsal cuticle. **C**. Granulation in the ventral body cuticle. **D**. Pores in the dorsal cuticle. **E**. Pores in the ventral cuticle. Scale bars in μm.

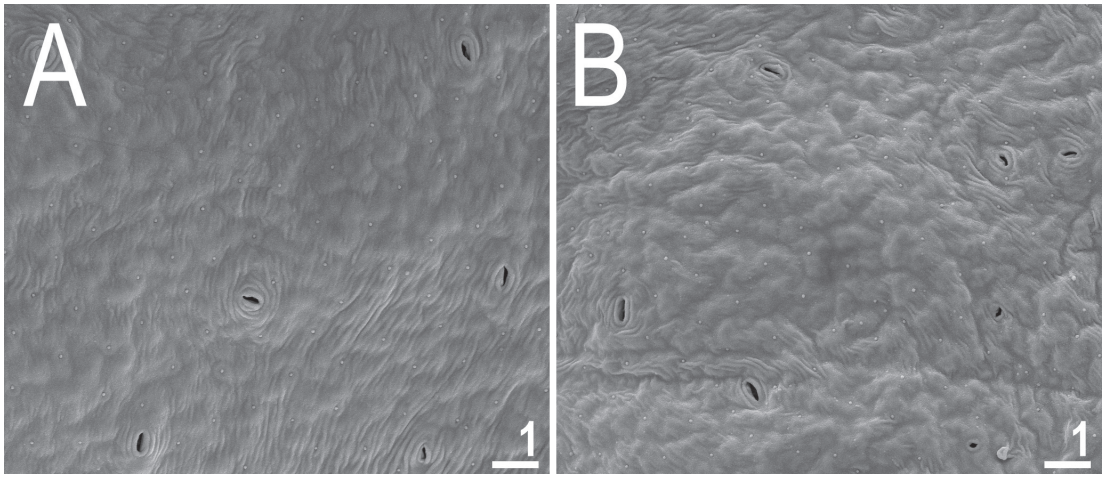

Fig. 2. *Macrobiotus ovovittatus* sp. nov., SEM images of body granulation and cuticular pores of a paratype (ISEA PAS). **A**. Body granulation and pores in the dorsal cuticle. **B**. Body granulation and pores in the ventral cuticle. Scale bars in μm.

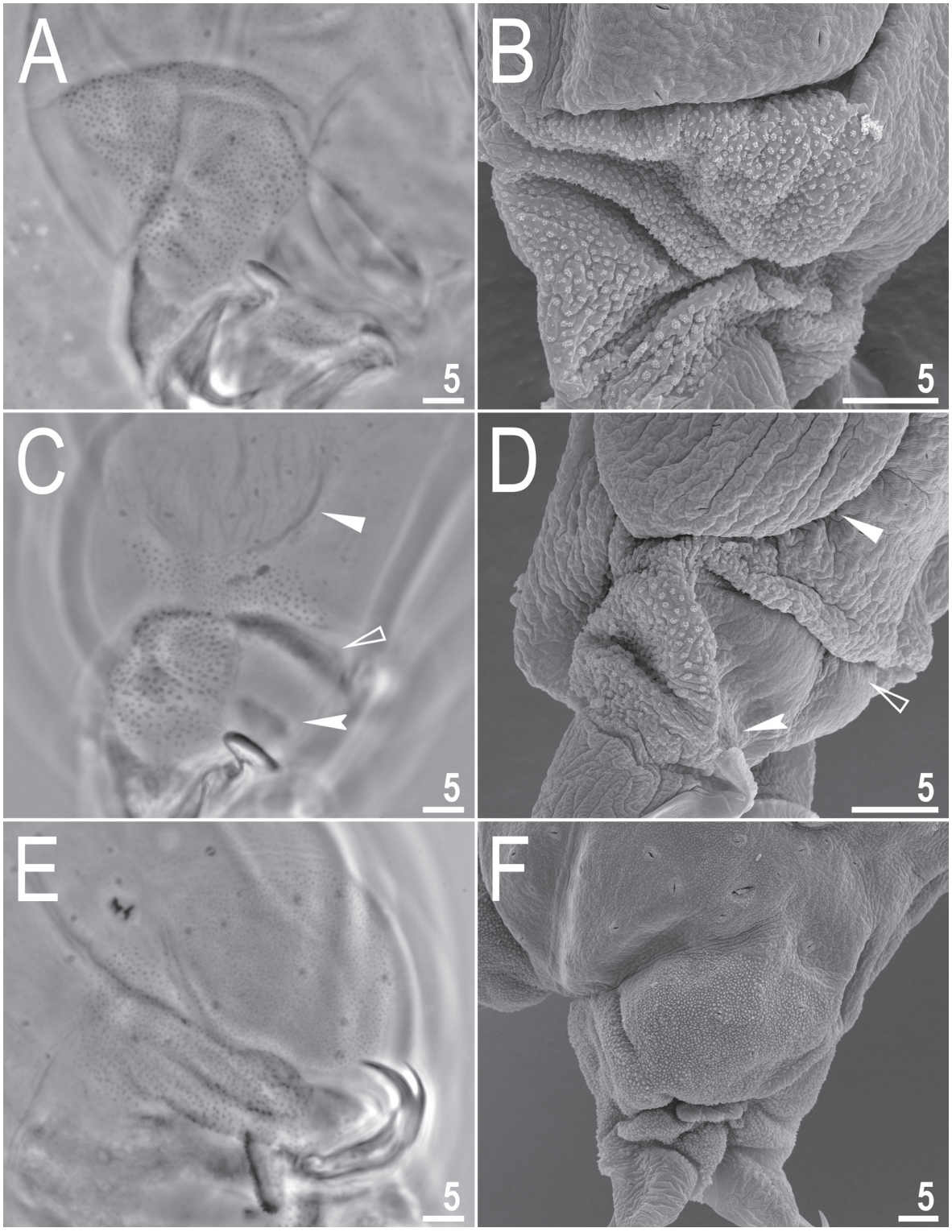

Fig. 3. *Macrobiotus ovovittatus* sp. nov., PCM (**A**, **C**, **E**) and SEM (**B**, **D**, **F**) images of dense granulation patches on legs of paratypes (ISEA PAS). **A**–**B**. Granulation on the external surface of leg III. **C**–**D**. Granulation on the internal surface of leg III and II, respectively. **E**–**F**. Granulation on the hind legs. The empty flat arrowheads indicate a single continuous cuticular bar above the claws, the filled flat arrowheads indicate a pulvinus-shaped cuticular bulge, and the filled indented arrowheads indicate shadowed extensions extending from the lunulae. Scale bars in μm.

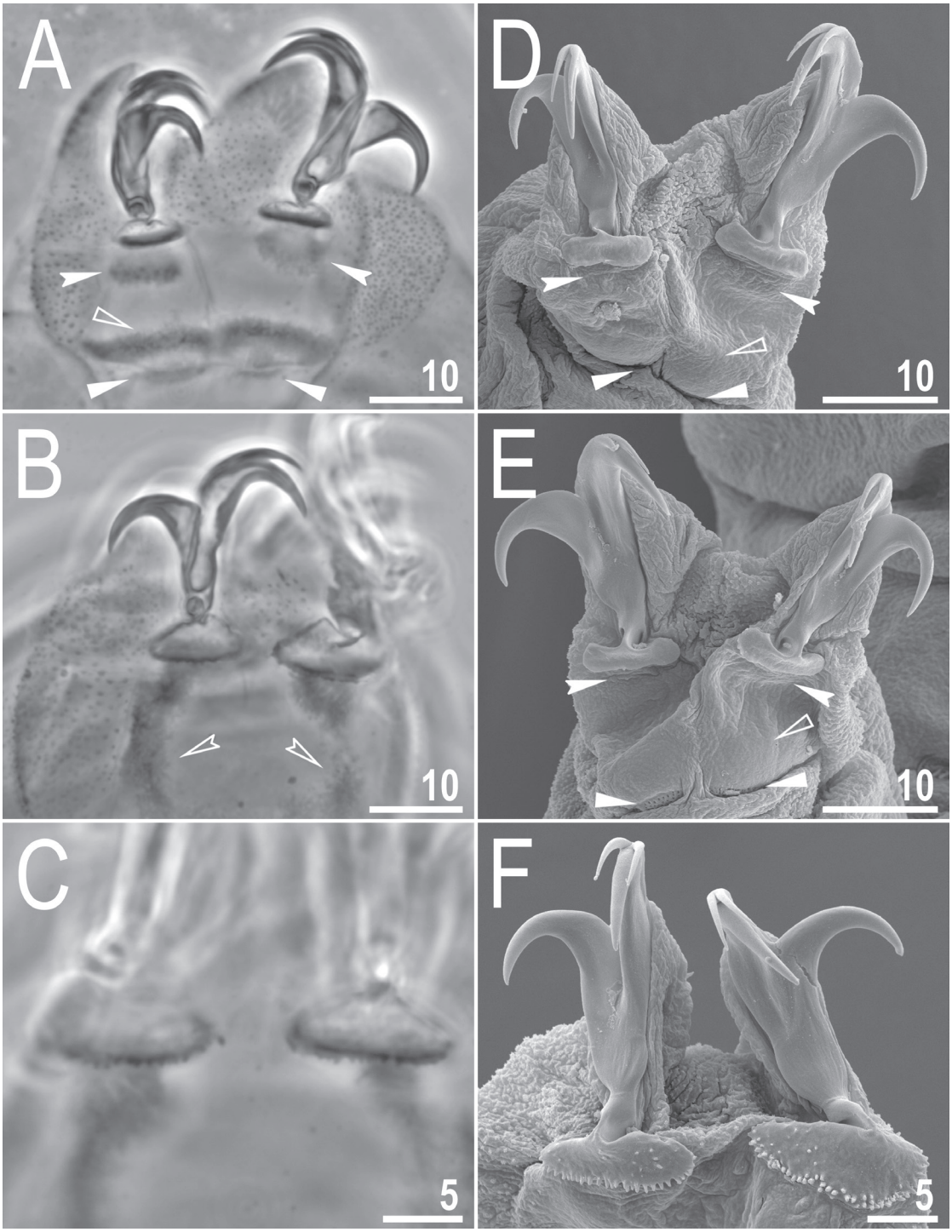

Figure 4. *Macrobiotus ovovittatus* sp. nov., images of claws. **A**–**C**. PCM, holotype (GL.001.01, ISEA PAS). **D**–**F**. SEM, paratype (ISEA PAS). **A**. Claws II with smooth lunulae. **B**. Claws IV with dentate lunulae. **C**. Dentate lunulae. **D**–**E**. Claws II and III with smooth lunulae, respectively. **F**. Claws IV with dentate lunulae. The empty flat arrowheads indicate a single continuous cuticular bar above the claws, the filled indented arrowheads indicate shadowed extensions extending from the lunulae (under PCM) or the places where they should be expected (SEM), the filled flat arrowheads indicate paired muscles attachments, and the empty indented arrowheads indicate the horseshoe structure connecting the anterior and the posterior claw. Scale bars in μm.

impression of incomplete reticulation (Fig. 7B, D, F). The processes are in the shape of inverted goblets with concave conical trunks and well-defined terminal discs (Figs 7A–H, 8A–F). Faint annulations are visible on the trunk of the process, especially in its distal portion, which is also covered by fine granulation (characters visible only under SEM; Fig. 8C–D). A crown of gently marked thickenings is visible around the bases of the processes as darker dots under PCM (Fig. 7B, D, F) and as thicker wrinkles at the processes bases under SEM (Fig. 8C–D). The terminal discs are cog-shaped, with a concave central area and 10–18 distinct teeth (Figs 7A–H, 8A–F). Terminal discs under PCM are covered by multiple light-refracting dots, and as such resemble crocheted napkins (Fig. 7A, C, E). These light refracting dots, when viewing the egg process laterally, give the impression that the terminal discs are rough and ragged (visible under PCM; Fig. 7 B, D, F–H). However, the terminal discs under SEM are

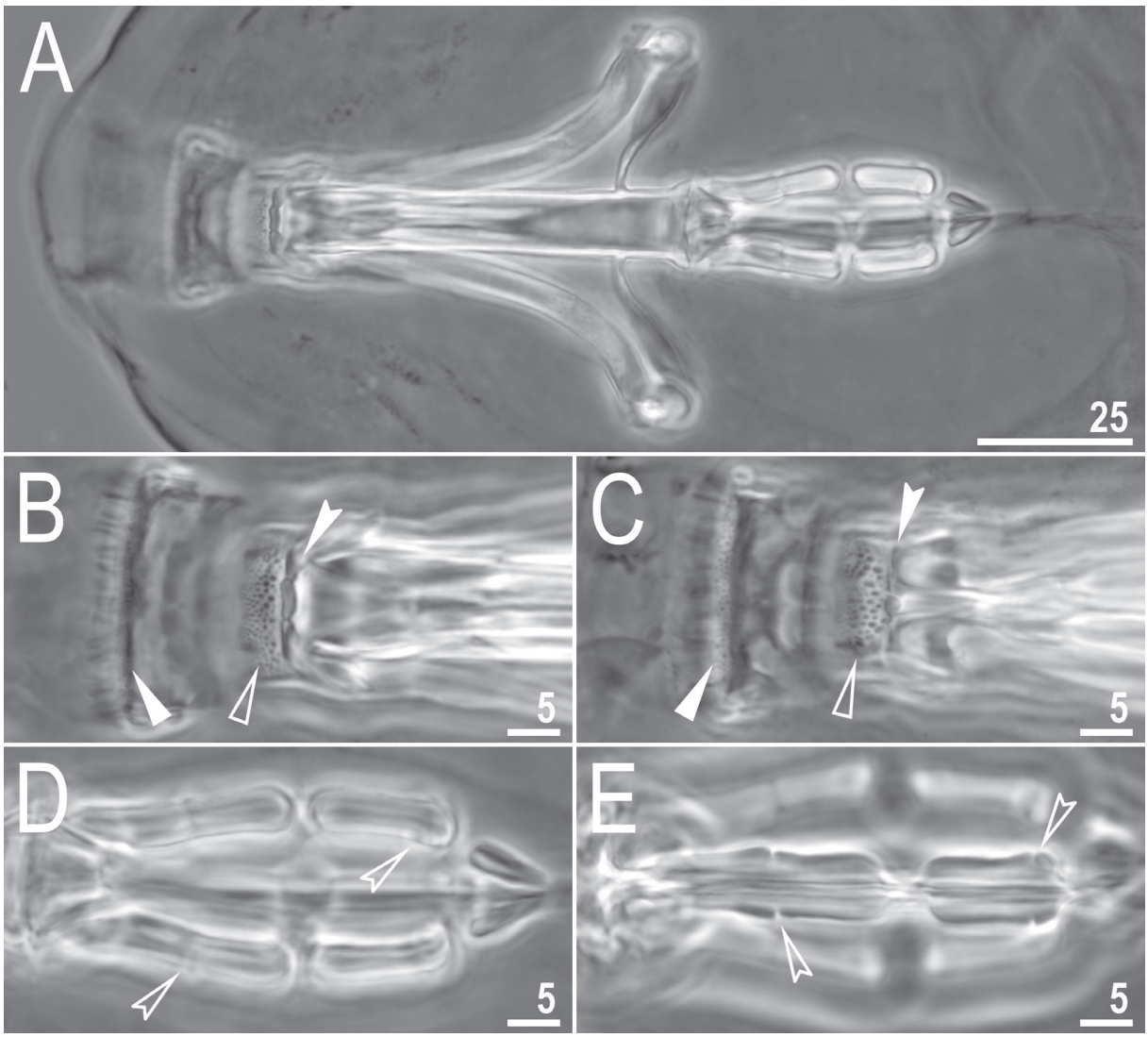

Fig. 5. *Macrobiotus ovovittatus* sp. nov., PCM images of the buccal apparatus, **A**–**D**. Holotype (GL.001.01, ISEA PAS). **E**. Paratype (ISEA PAS). **A**. An entire buccal apparatus. **B**–**C**. The oral cavity armature, dorsal and ventral teeth, respectively. **D**–**E**. Placoid morphology, dorsal and ventral placoids respectively. The filled flat arrowheads indicate the first band of teeth, the empty flat arrowheads indicate the second band of teeth, the filled indented arrowheads indicate the third band of teeth, and the empty indented arrowheads indicate central and subterminal constrictions in the first and second macroplacoid, respectively. Scale bars in μm.

Table 2. Measurements [in µm] and *pt* values of selected morphological structures of animals of *Macrobiotus ovovittatus* sp. nov.; specimens mounted in Hoyer's medium; N: number of specimen/ structures measured; range: refers to the smallest and the largest structure among all measured specimens; SD: standard deviation.

Character	N	Range		Mean		SD		Holotype	
		µm	*pt*	µm	*pt*	µm	*pt*	µm	*pt*
Body length	20	570–879	*981–1249*	726	*1120*	95	*67*	757	*1083*
Buccal tube									
Buccal tube length	20	54.5–75.3	–	64.6	–	5.6	–	69.9	–
Stylet support insertion point	20	44.7–60.8	*80.1–82.4*	52.4	*81.1*	4.5	*0.6*	56.4	*80.7*
Buccal tube external width	20	7.9–13.4	*14.5–18.5*	10.6	*16.4*	1.4	*1.0*	11.6	*16.6*
Buccal tube internal width	20	5.9–10.5	*10.8–13.9*	8.1	*12.5*	1.1	*0.8*	8.5	*12.2*
Ventral lamina length	20	33.1–48.2	*60.0–68.7*	41.5	*64.2*	4.4	*2.9*	46.6	*66.7*
Placoid lengths									
Macroplacoid 1	20	15.5–24.3	*28.4–34.4*	20.3	*31.3*	2.6	*1.8*	22.8	*32.6*
Macroplacoid 2	20	10.1–17.0	*18.2–22.6*	13.1	*20.2*	1.9	*1.4*	13.4	*19.2*
Microplacoid	20	6.3–9.6	*9.3–13.5*	7.5	*11.6*	1.0	*1.0*	8.4	*12.0*
Macroplacoid row	20	27.1–43.3	*48.5–59.0*	35.3	*54.4*	4.8	*3.0*	38.9	*55.7*
Placoid row	20	35.2–55.1	*62.7–75.2*	44.5	*68.6*	5.7	*3.2*	49.6	*71.0*
Claw I heights									
External primary branch	19	13.7–21.7	*24.6–29.3*	17.4	*26.8*	2.2	*1.5*	17.5	*25.0*
External secondary branch	18	10.5–15.5	*18.7–23.5*	13.7	*21.1*	1.4	*1.1*	14.7	*21.0*
Internal primary branch	19	12.4–19.8	*22.1–26.3*	15.9	*24.7*	1.8	*1.1*	16.9	*24.2*
Internal secondary branch	18	10.5–14.5	*17.5–21.6*	12.5	*19.6*	1.2	*1.0*	14.1	*20.2*
Claw II heights									
External primary branch	20	13.6–21.4	*25.0–30.7*	18.0	*27.8*	2.2	*1.5*	19.9	*28.5*
External secondary branch	15	10.9–16.9	*19.7–24.1*	14.1	*22.1*	1.8	*1.4*	16.7	*23.9*
Internal primary branch	20	11.9–20.9	*21.8–27.8*	16.3	*25.2*	2.1	*1.5*	17.3	*24.7*
Internal secondary branch	19	9.3–17.2	*17.1–22.8*	13.2	*20.3*	1.8	*1.6*	14.3	*20.5*
Claw III heights									
External primary branch	20	14.5–23.2	*26.4–30.8*	18.3	*28.2*	2.2	*1.3*	19.5	*27.9*
External secondary branch	18	12.3–18.4	*21.5–25.0*	15.0	*23.1*	1.6	*1.0*	16.2	*23.2*
Internal primary branch	20	13.2–19.9	*23.5–27.0*	16.5	*25.5*	1.8	*1.0*	17.7	*25.3*
Internal secondary branch	17	11.2–16.5	*18.4–22.1*	13.4	*20.8*	1.5	*1.1*	15.2	*21.7*
Claw IV heights									
Anterior primary branch	20	16.1–25.1	*28.0–33.6*	19.6	*30.2*	2.4	*1.6*	19.6	*28.0*
Anterior secondary branch	15	12.5–17.5	*20.9–24.9*	15.0	*23.0*	1.6	*1.1*	15.6	*22.3*
Posterior primary branch	20	17.1–27.0	*30.7–35.9*	20.9	*32.3*	2.5	*1.5*	21.7	*31.0*
Posterior secondary branch	10	13.5–18.9	*21.9–25.3*	15.6	*23.9*	1.6	*1.2*	16.2	*23.2*

solid without any pores or light refracting dots, their teeth, are covered by small granules (visible only under SEM) that probably serve to improve the adhesive properties of the egg processes (Fig. 8C–F). The measurements and statistics of eggs are given in Table 3.

Reproduction

The reproduction mode of *M. ovovittatus* sp. nov. is unknown. Examination of orcein-stained specimens revealed no spermatozoa, but only developing oocytes. The same was true for the observation of freshly mounted individuals in Hoyer's medium that did not reveal any sperm either but only developing oocytes. Therefore, this population could be parthenogenetic or hermaphroditic (considering its close relationship with hermaphroditic taxa in Fig. 21). In the second case, it might have been possible that there were no specimens in the development stage when the sperm could be detectable.

Differential diagnosis

By having (i) three bands of teeth in the oral cavity armature that are well visible under light microscope, (ii) entire body cuticle covered by granulation (sometimes visible only under SEM), (iii) eggs with inverted goblet shaped processes, the new species is the most similar to four other taxa of *Macrobiotus*, namely *Macrobiotus joannae* Pilato & Binda, 1983 reported from its type locality in Australia (Pilato & Binda 1983), and several uncertain localities in central, eastern, and southeastern Russia (Biserov 1990) and from Italy (Bertolani *et al.* 2014), *Macrobiotus hannae* Nowak & Stec, 2018 known only from its type locality in Poland (Nowak & Stec 2018), *Macrobiotus punctillus* Pilato, Binda & Azzaro, 1990 known only from its type locality in Chile (Pilato *et al.* 1990) and *Macrobiotus rebecchii* Stec, 2022 known only from its type locality in Kyrgyzstan (Stec 2022b). However, it can be easily distinguished from all of them by having a different morphology of the egg surface (the surface is continuous/solid and clearly wrinkled with sparse, very small and irregularly spaced pores in the new species vs chorion surface covered by evident reticulum in the other species), a different appearance of the terminal discs under PCM (the terminal discs are covered by multiple light-refracting dots, and as such resemble crocheted napkins vs terminal discs without light-refracting dots in other species).

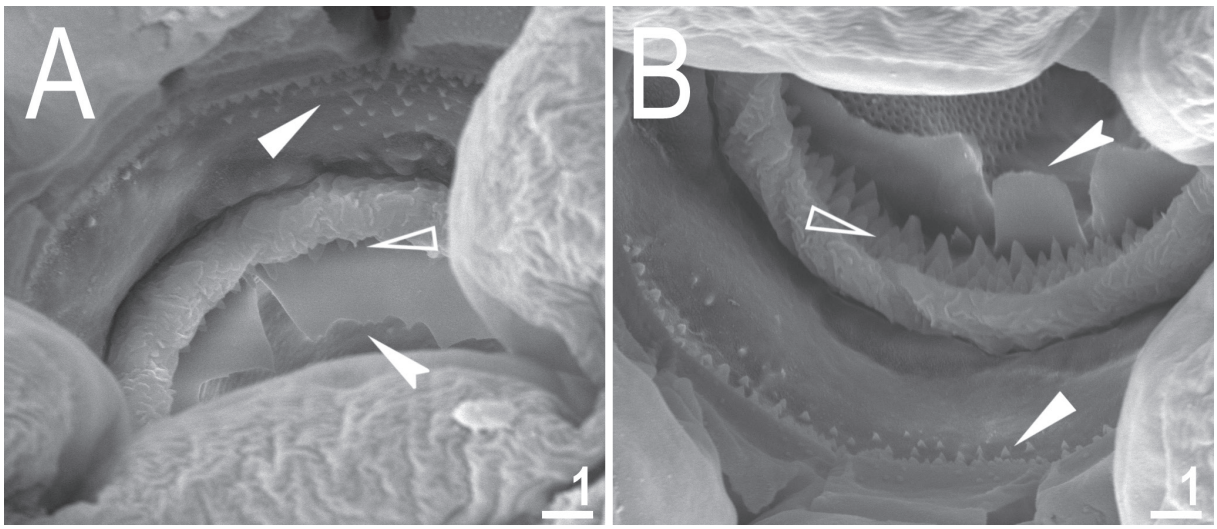

Fig. 6. *Macrobiotus ovovittatus* sp. nov., mouth opening and the oral cavity armature of a single paratype (ISEA PAS) seen under SEM from different angles. **A**. Dorsal view. **B**. Ventral view. The filled flat arrowheads indicate the first band of teeth, the empty flat arrowheads indicate the second band of teeth, and the filled indented arrowheads indicate the third band of teeth. Scale bars in μm.

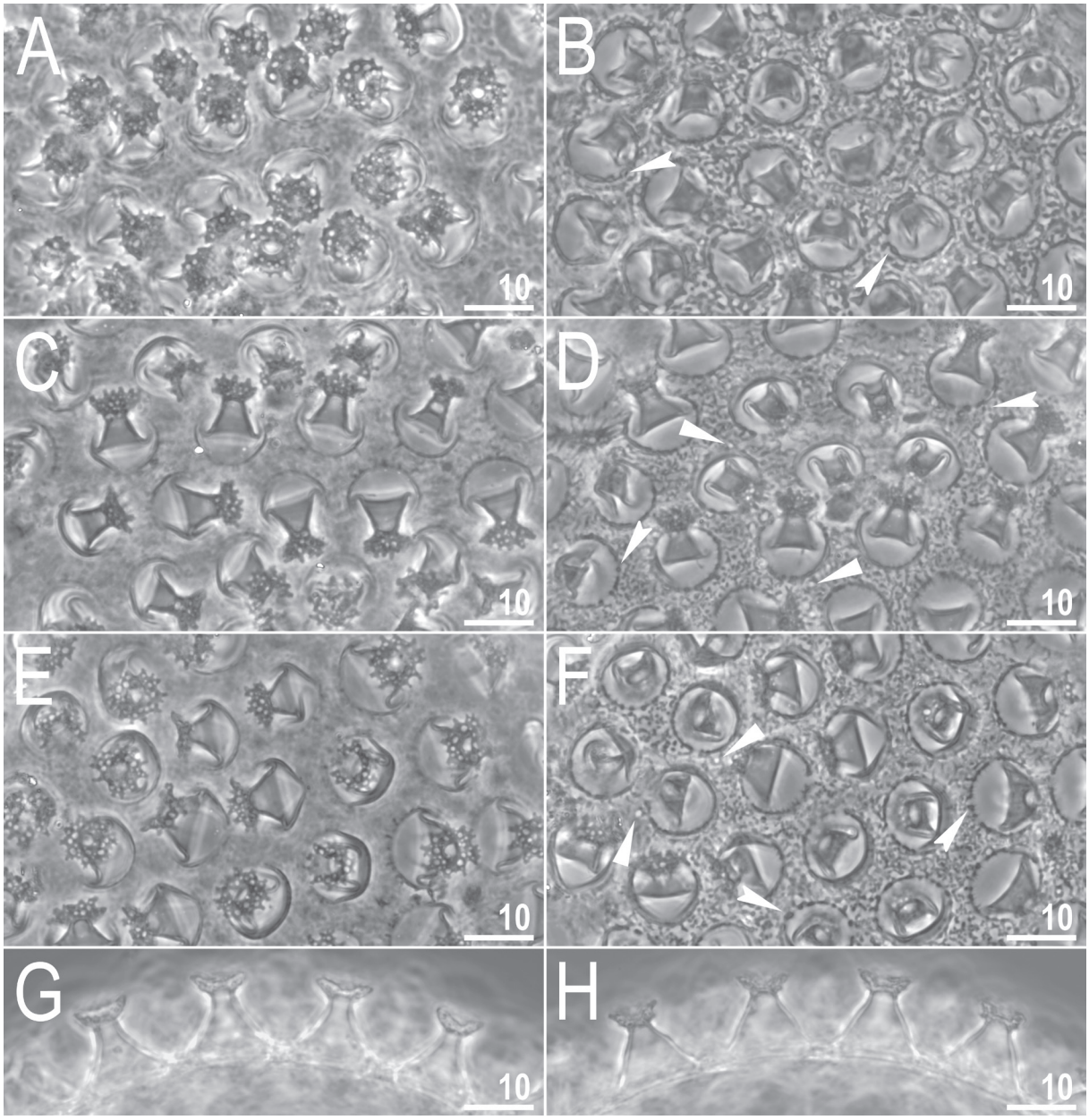

Fig. 7. *Macrobiotus ovovittatus* sp. nov., PCM images of the eggs (ISEA PAS) under ×1000 magnification. **A**, **C**, **E**. Egg surface with focus on egg processes and terminal discs. **B**, **D**, **F**. Egg surface, focus on the surface between processes. **G**–**H**. Midsections of egg processes. The filled indented arrowheads indicate thickenings around the process bases and filled flat arrowheads indicate faintly visible pores. Scale bars in μm.

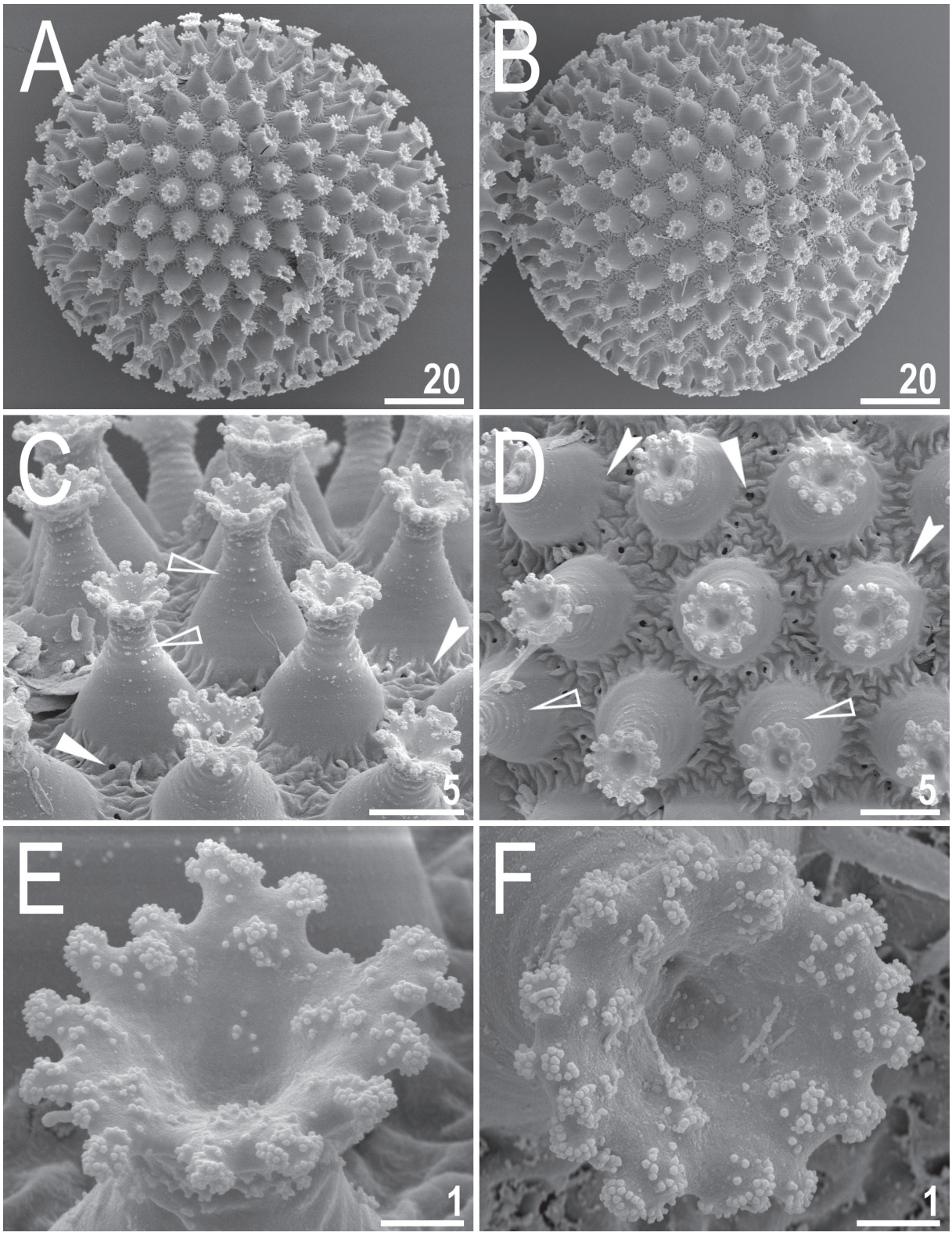

Fig. 8. *Macrobiotus ovovittatus* sp. nov., SEM images of eggs (ISEA PAS). **A**–**B**. Entire egg. **C**–**D**. Details of egg processes and the surface between them. **E**–**F**. Details of the terminal disc. The filled indented arrowheads indicate thickenings around the process bases and filled flat arrowheads indicate faintly visible pores. Scale bars in μm.

Table 3. Measurements [in μm] of the eggs of *Macrobiotus ovovittatus* sp. nov.; eggs mounted in Hoyer's medium; process base/height ratio is expressed as percentage; N: number of eggs/structures measured; range: refers to the smallest and the largest structure among all measured specimens; SD: standard deviation.

Character	N	Range	Mean	SD
Egg bare diameter	9	100.6–129.8	117.6	12.8
Egg full diameter	9	125.5–155.4	142.2	12.6
Process height	27	9.5–13.5	11.9	0.9
Process base width	27	9.4–13.6	11.1	0.9
Process base/height ratio	27	78%–115%	95%	11%
Terminal disc width	27	6.1–8.7	7.4	0.7
Inter-process distance	27	2.2–4.1	3.4	0.5
Number of processes on the egg circumference	9	28–34	31.2	2.2

Macrobiotus mileri sp. nov.
urn:lsid:zoobank.org:act:99372E2F-595A-4AB2-8398-21198A2CBD7E
Figs 9–20, Tables 4–5

Etymology

The species is named in honour of Krzysztof Miler, who has developed an impressive tolerance for the daily tardigrade madness that surrounds him.

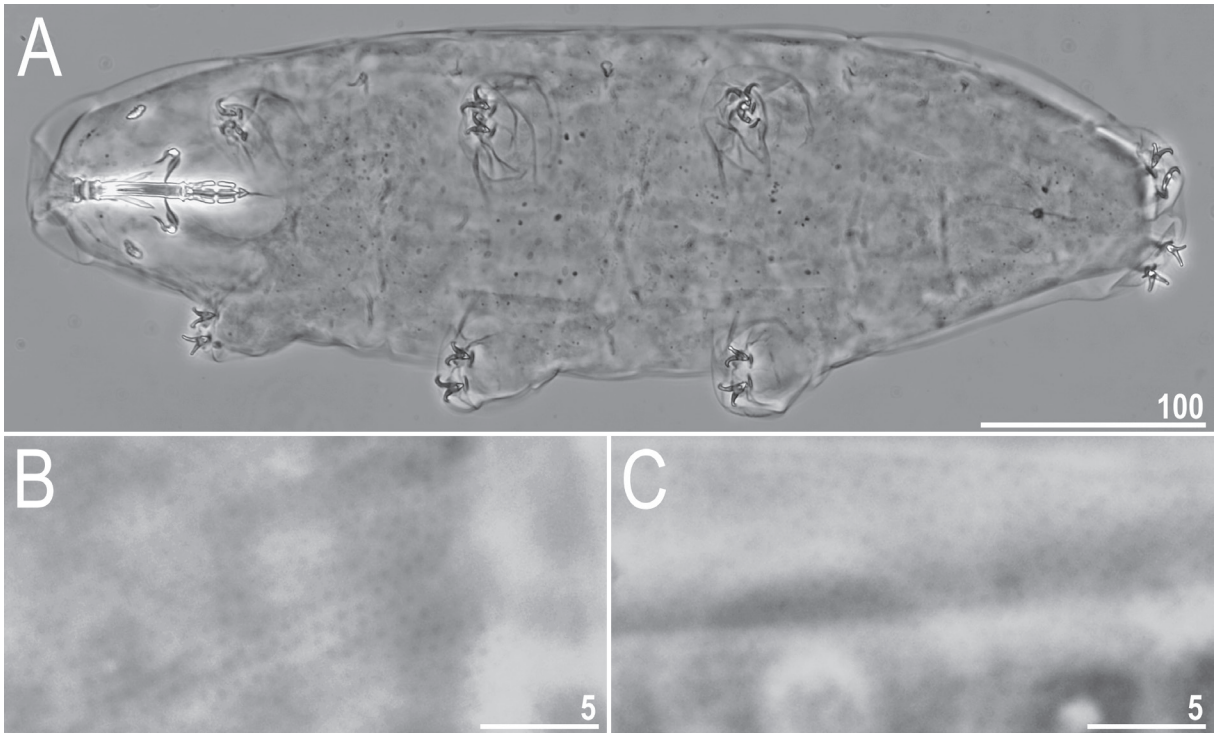

Fig. 9. *Macrobiotus mileri* sp. nov., PCM images of habitus and body granulation. **A**. Dorso-ventral projection (holotype, IL.001.11, ISEA PAS, forma aporata). **B**. Granulation in the dorsal cuticle (paratype, ISEA PAS, forma aporata). **C**. Granulation in the dorsal body cuticle (paratype, ISEA PAS, forma porata). Scale bars in μm.

Material examined

39 animals, 7 eggs mounted on microscope slides in Hoyer's medium, 7 animals and 3 eggs examined under SEM, and 4 animals processed for DNA sequencing.

Type material

Holotype

ISRAEL • Tel-Aviv; 32°2′42.82″ N, 34°46′14.88″ E; 19 m a.s.l.; Nov. 2019; K. Miler leg.; moss growing on a stone wall in urban park; ISEA PAS, slide IL.001.11.

Paratypes

ISRAEL • 45 animals; same collection data as for the holotype; ISEA PAS, slides IL.001.08 to IL.001.12, SEM stub TAR.014 • 10 eggs; same collection data as for the holotype; ISEA PAS, slides IL.001.06 to IL.001.07, SEM stub TAR.014.

Description

Animals

Body transparent in juveniles and white in adults, after fixation in Hoyer's medium transparent (Fig. 9A). Eyes present. Granulation is present on the entire body cuticle and is visible under PCM and SEM, but granulation on the ventral side of the body is less dense (Figs 9B–C, 10A–F). In terms of cuticular pores, two morphological forms of animals are present in this species. One form (forma porata) with large, evident pores arranged specifically in five patches (Figs 11A–B, 12A–D, 13) and second form (forma aporata) with only small, single pores randomly distributed on the body (almost indetectable under PCM and hardly detectable also under SEM; 0.2–0.4 μm in diameter; Figs 10E–F, 14A, 16C, 18A–B). In forma porata, the round and oval pores (0.4–0.7 μm in diameter) are arranged into five distinct patches: (I) a sparse patch of pores on the external surface of the distal portion of leg I (Figs 13, 15A); (II) a dense patch of pores on the external surface of the proximal portion of leg II extending also towards the lateral body cuticle (Figs 11A, 13); (III) a dense patch of pores on the lateral body surface between legs II and II (Figs 11A, 12A, C, 13); (IV) a dense large patch of pores covering the whole external surface of leg III, extending also towards the lateral body cuticle (Figs 11A–B, 12A, C, 13); and (V) the largest patch of pores that extends from the left caudo-lateral surface, through the dorsal caudal surface to the right caudo-lateral surface, extending also towards lateral and dorsal surfaces of legs IV (Figs 11B, 12A–D, 13, 15D). Only the V patch is single and continuous, while patches I–IV are doubled and present symmetrically on each side of the body. In both forms, some evident dense granulation patches are visible on the external and internal surfaces of all legs I–III, as well as on the lateral and dorsal surfaces of legs IV under PCM and SEM (Figs 14A–D, 15A–D). Small pores, visible only under SEM, can be seen in between the granulation on the hind legs (Fig. 15D). A pulvinus-shaped cuticular bulge is not visible on the internal surface of legs I–III, but there is a garter-shaped structure on the external surface of all legs I–III (Figs 13, 14A–B, 15A–B) above which there is a small cuticular bulge / fold (visible only under SEM; Fig. 15A–B).

Small and robust *hufelandi*-type claws (Fig. 16A–E). Primary branches with distinct accessory points, a moderately long common tract, and an evident stalk connecting the claw to the lunula (Fig. 16A–F). The lunulae on legs I–III are smooth (Fig. 16A, D), while there is dentation in the lunulae on legs IV (Fig. 16B, C, E). The cuticular bars are absent, but double muscle attachments are present above the claws I–III (Fig. 16A, D). Shadowed extensions extending from lunulae on legs I–III are present and faintly visible only under PCM (Fig. 16A). A horseshoe-shaped structure connects the anterior and posterior lunules on leg IV (Fig. 16C).

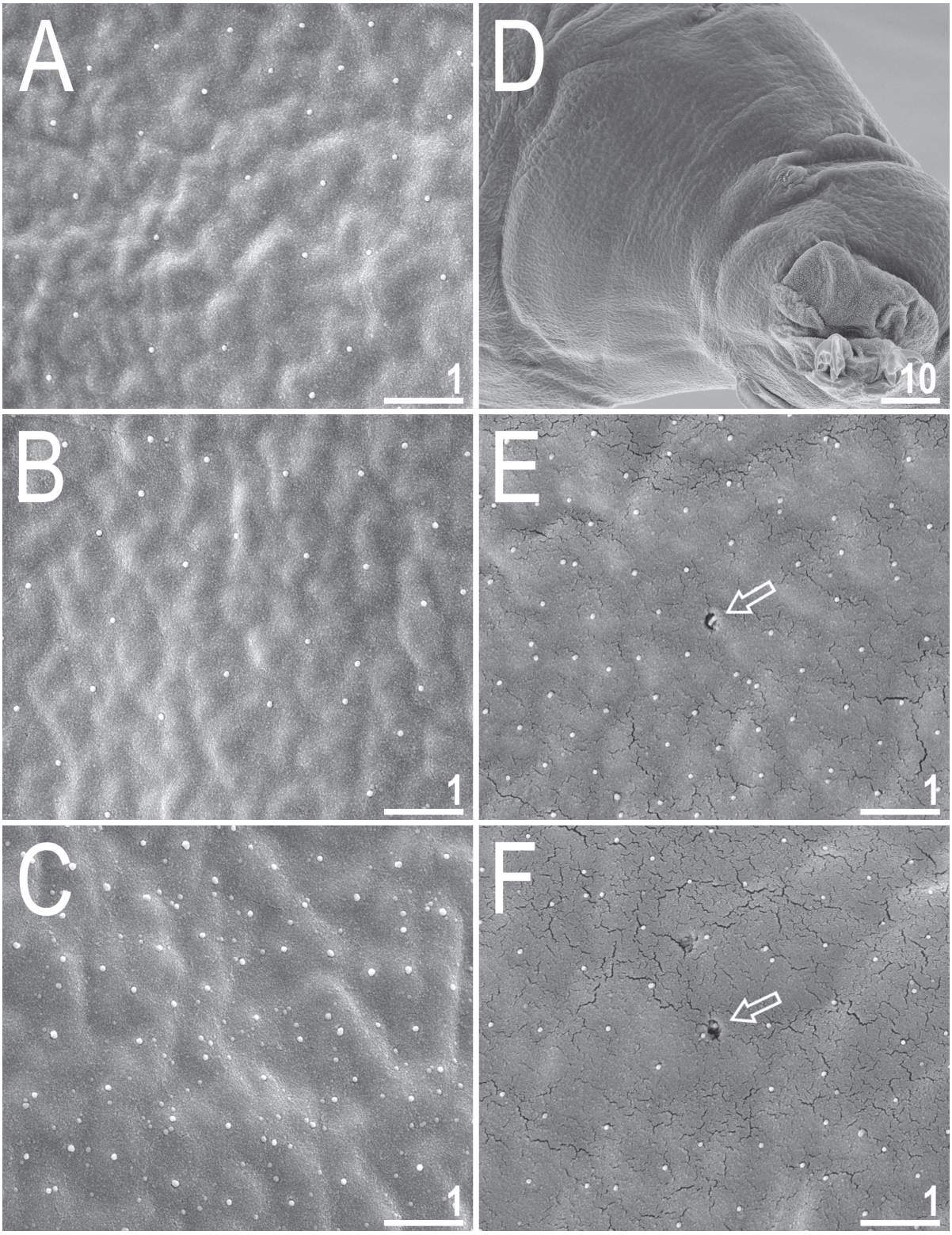

Fig. 10. *Macrobiotus mileri* sp. nov., SEM images of body granulation and cuticular pores (paratype, ISEA PAS, forma aporata). **A**. Body granulation in the dorsal head region. **B**. Body granulation in the dorsal central body region. **C**. Body granulation in the dorsal caudal body region. **D**. General view of body granulation in the lateral caudal body region. **E–F**. Singular pores in the body cuticle. Scale bars in μm.

Mouth antero-ventral. Bucco-pharyngeal apparatus of *Macrobiotus* type, with ventral lamina and ten small peribuccal lamellae followed by six buccal sensory lobes (Figs 17A, 18A–D). Under PCM, the oral cavity armature is of *hufelandi* type – three bands of teeth are always visible (Fig. 17B–C). The first band of teeth is composed of numerous extremely small cones arranged in four to six rows located anteriorly in the oral cavity, just behind the bases of the peribuccal lamellae (Figs 17B–C, 18C–D). The second band of teeth is located between the ring fold and the third band of teeth and comprises about four rows of small cones, larger than those of the first band (Figs 17B–C, 18C–D). The teeth of the third band are located within the posterior portion of the oral cavity, between the second band of teeth and the opening of the buccal tube (Figs 17B–C, 18C–D). The third band of teeth is discontinuous

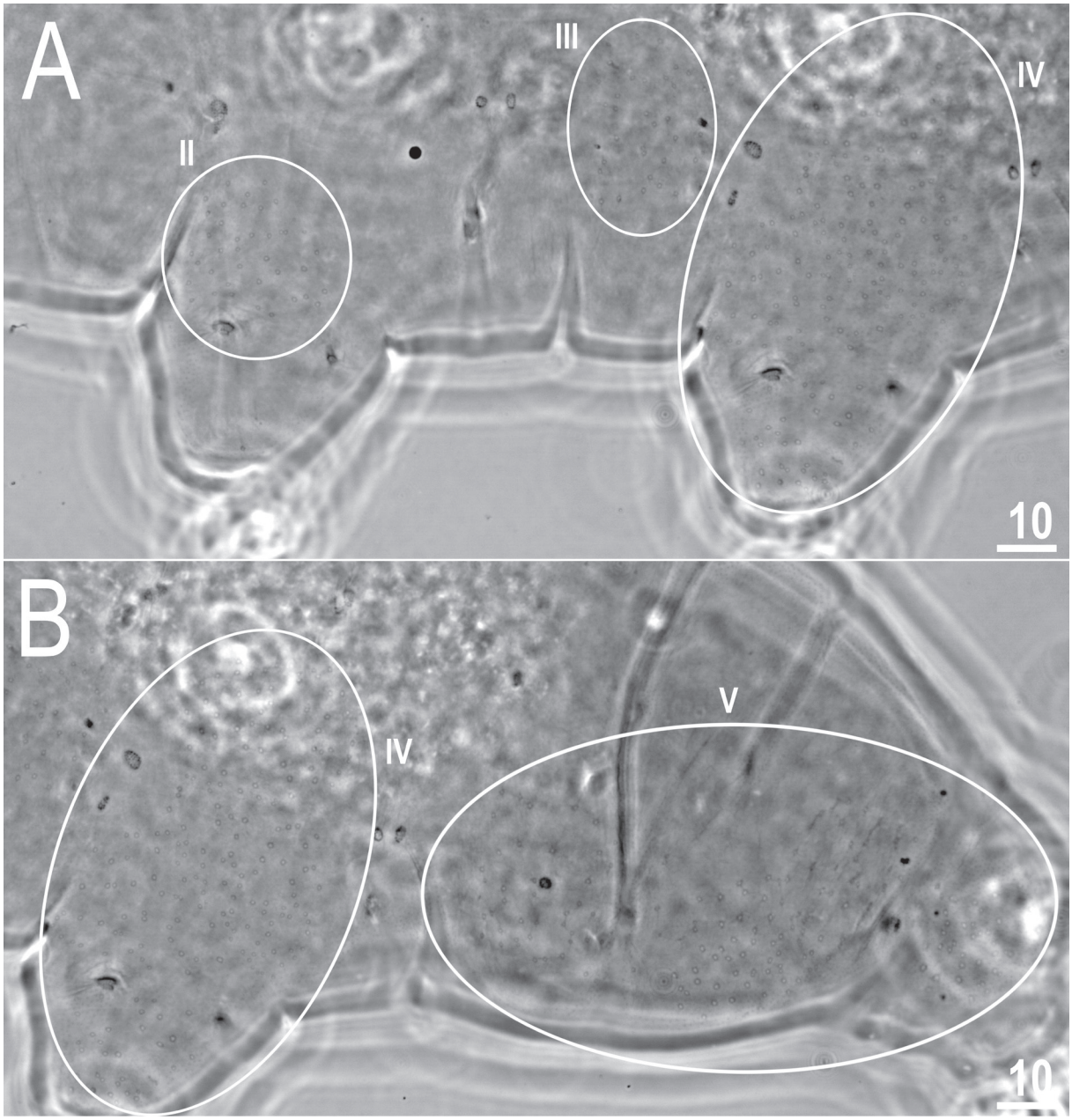

Fig. 11. *Macrobiotus mileri* sp. nov., PCM images of cuticular pores patches in forma porata (paratype, ISEA PAS). **A**. Patches II, III and IV. **B**. Patches IV and V. Scale bars in μm.

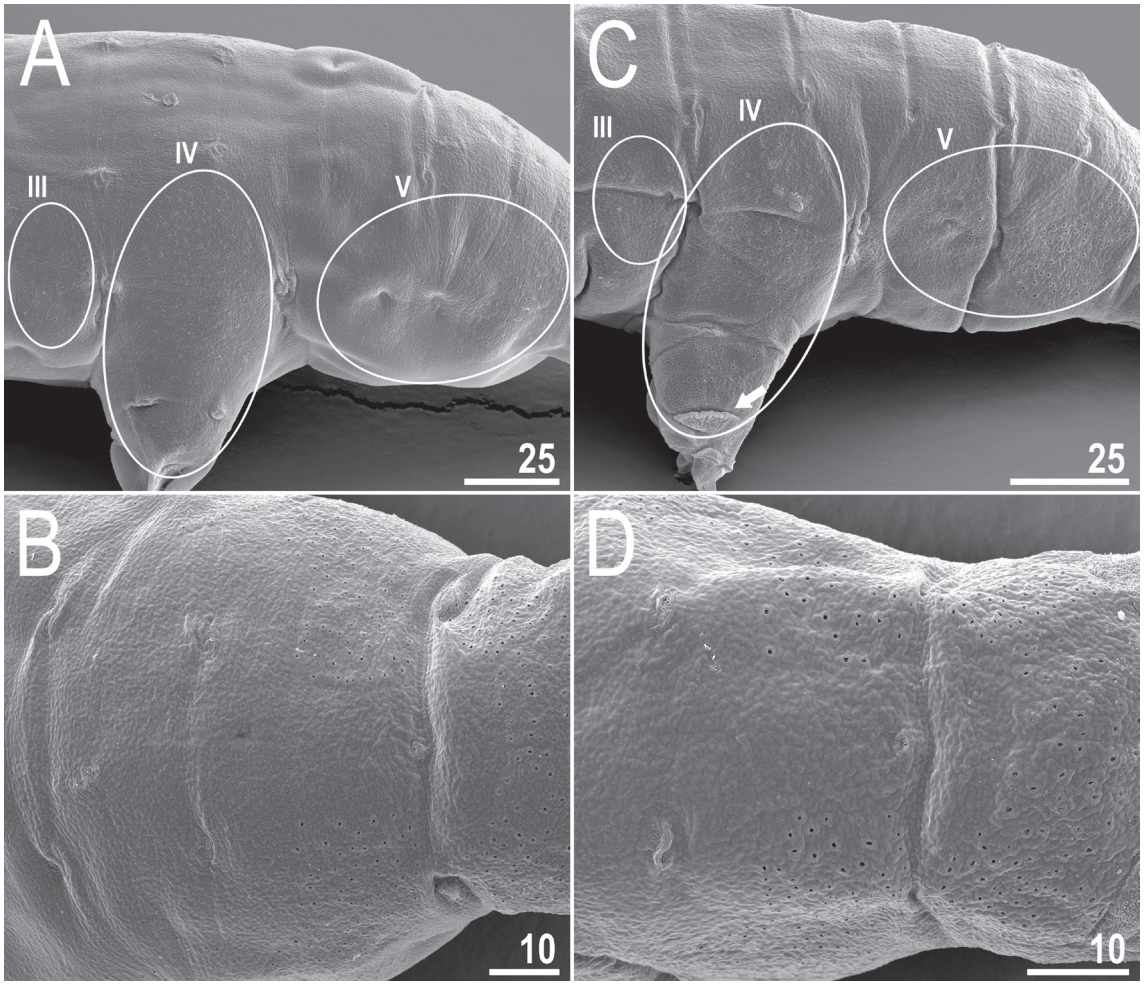

Fig. 12. *Macrobiotus mileri* sp. nov., SEM images of cuticular pores patches in two paratypes of forma porata (ISEA PAS). **A**, **C**. Patches II, III and IV. **B**, **D**. Dorsal view on the caudal body region with continuous patch V of pores. Scale bars in μm.

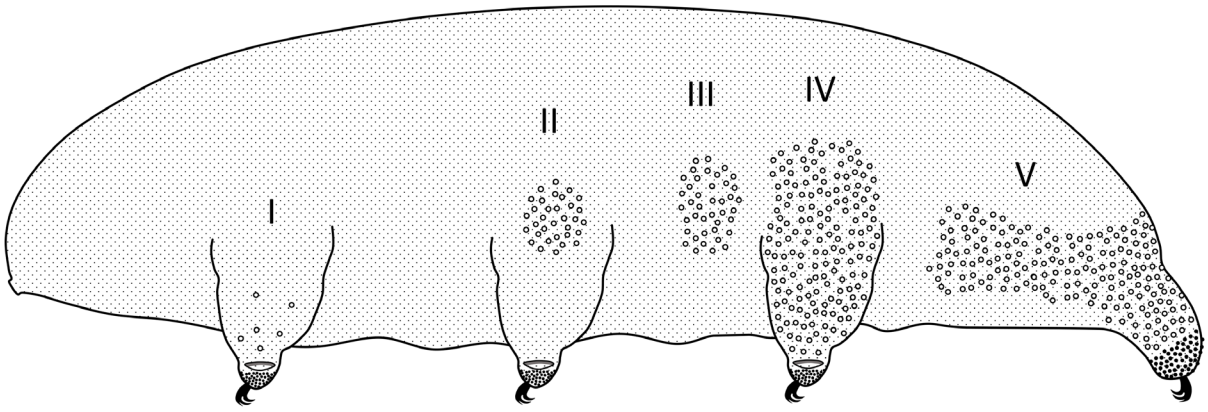

Fig. 13. *Macrobiotus mileri* sp. nov., a schematic drawing of a specimen belonging to forma porata, showing the distribution of patches of cuticular pores, body and leg granulation as well as the garter-shaped structures on legs I–III.

and divided into the dorsal and ventral portions. Under PCM, dorsal teeth are seen as three distinct transverse ridges, and the medio-dorsal tooth is evidently longer than the latero-dorsal teeth (Fig. 17B). The ventral teeth appear as two separate lateral transverse ridges between which a median tooth is visible and rarely divided into two teeth (Fig. 17C). Under SEM, the dorsal and ventral teeth are also clearly distinct (Fig. 18C–D). Under SEM, the margins of the dorsal teeth are serrated and the medio-dorsal tooth is clearly longer than latero-dorsal teeth (Fig. 18C) whereas the ventral teeth are smaller and their margins are less serrated (Fig. 18D). Pharyngeal bulb spherical, with triangular apophyses, two rod-shaped macroplacoids and a large triangular microplacoid (Fig. 17A). The macroplacoid length sequence being 2 <1. The first and the second macroplacoid are constricted centrally and subterminally, respectively (Fig. 17D–E). The animals' measurements and statistics are given in Table 4.

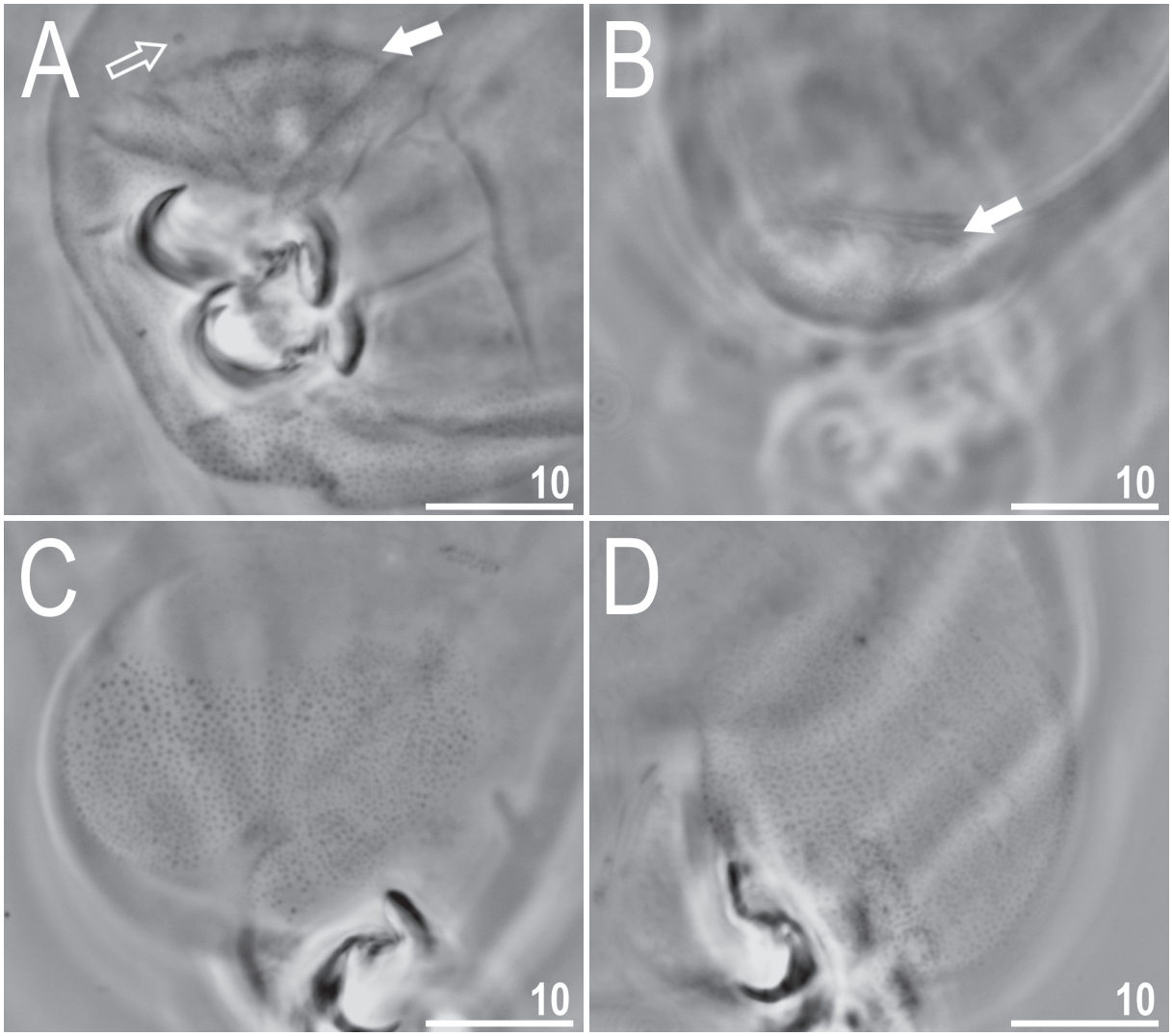

Fig. 14. *Macrobiotus mileri* sp. nov., PCM images of dense granulation patches and cuticular structures on legs (paratypes, ISEA PAS). **A**. Granulation on the external, proximal and internal surface of leg II. **B**. Garter-shaped structure and granulation on the external surface of leg II. **C**. Granulation on the internal surface of leg III. **D**. Granulation on the hind leg. The empty arrow indicates a cuticular pore, filled arrows indicate the garter-shaped structure. All photographs taken from specimens belonging to forma aporata; scale bars in μm.

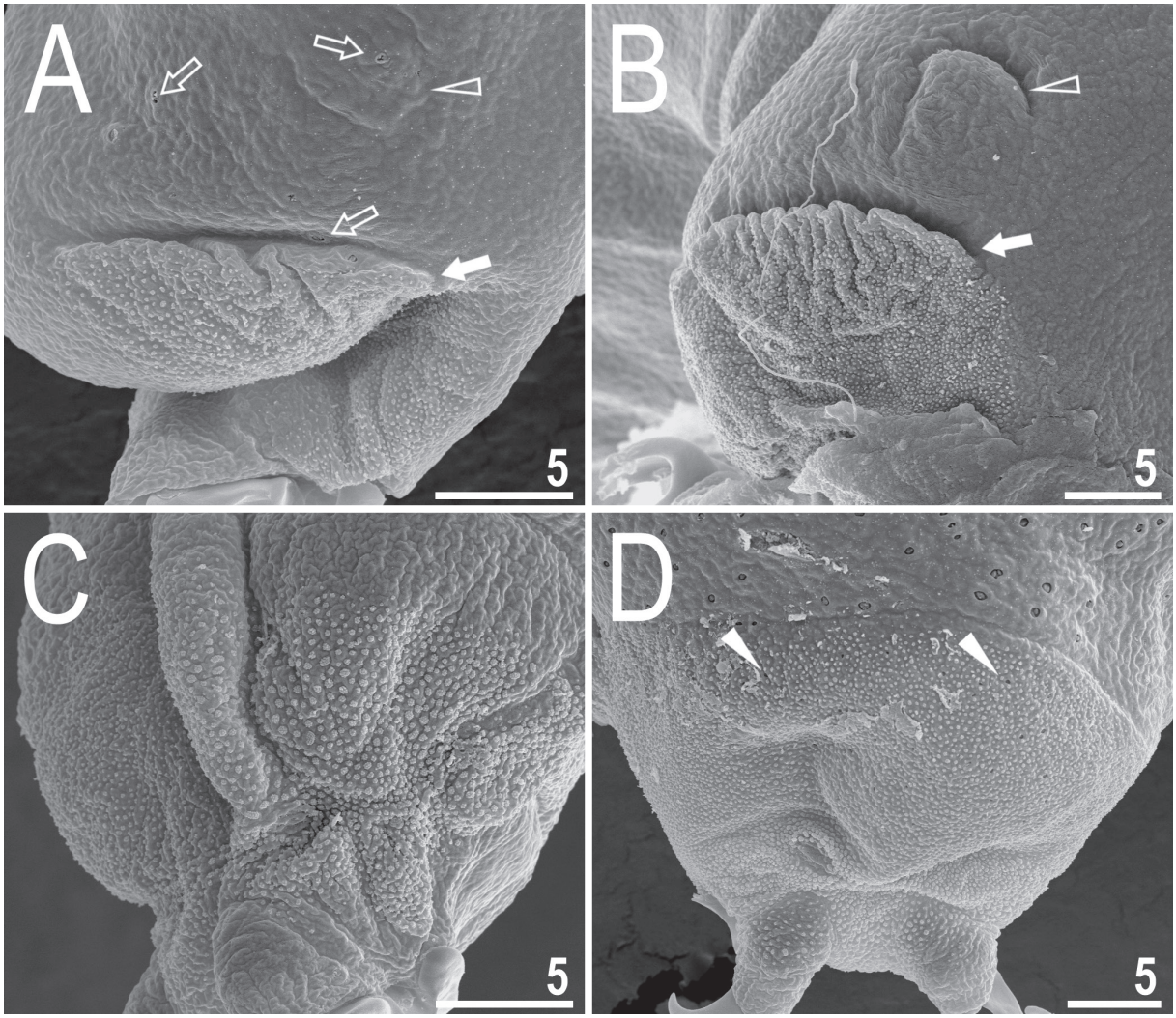

Fig. 15. *Macrobiotus mileri* sp. nov., SEM images of dense granulation patches and cuticular structures on legs (paratypes, ISEA PAS). **A**. Granulation and garter-shaped structure on the external surface of leg I (forma porata). **B**. Granulation and garter-shaped structure on the external surface of leg II (forma aporata). **C**. Granulation on the internal surface of leg II (forma porata). **D**. Granulation on the hind leg (forma porata). Empty arrows indicate cuticular pores, filled arrows indicate the garter-shaped structure, empty flat arrowheads indicate the small cuticular bulge / fold, filled flat arrowheads indicate small pores in between granulation that are visible only under SEM. Scale bars in μm.

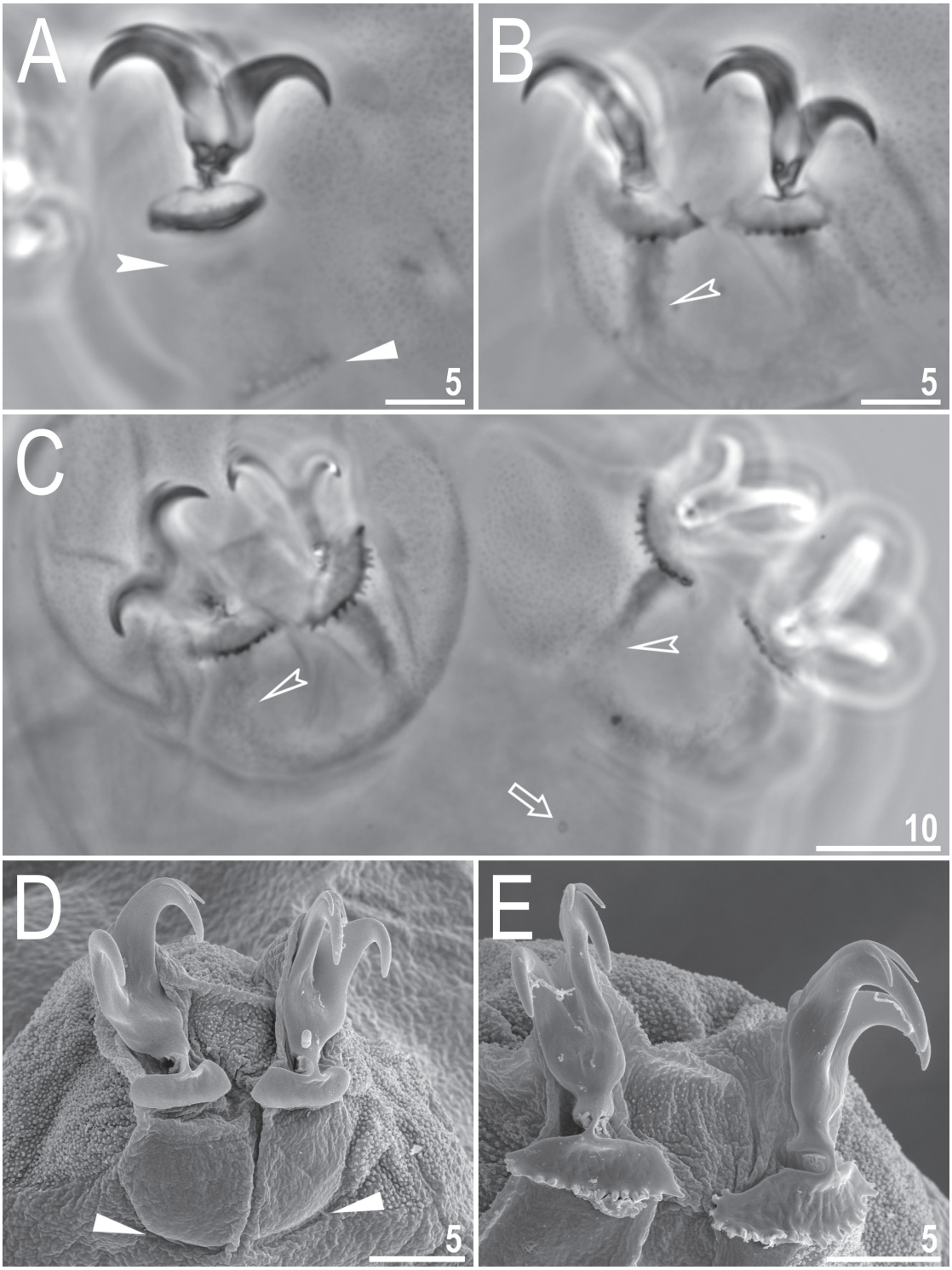

Fig. 16. *Macrobiotus mileri* sp. nov., images of claws (paratypes, ISEA PAS). **A**. Claws II with smooth lunulae (PCM, forma aporata). **B**. Claws IV with dentate lunulae (PCM, forma aporata). **C**. Dentate lunulae (PCM, forma aporata). **D**. Claws II with smooth lunulae, respectively (SEM, forma porata). **E**. Claws IV with dentate lunulae (SEM, forma porata). The empty arrow indicates a singular cuticular pore, filled indented arrowheads indicate shadowed extensions extending from the lunulae (under PCM), filled flat arrowheads indicate paired muscles attachments, and empty indented arrowheads indicate the horseshoe structure connecting the anterior and the posterior claw. Scale bars in μm.

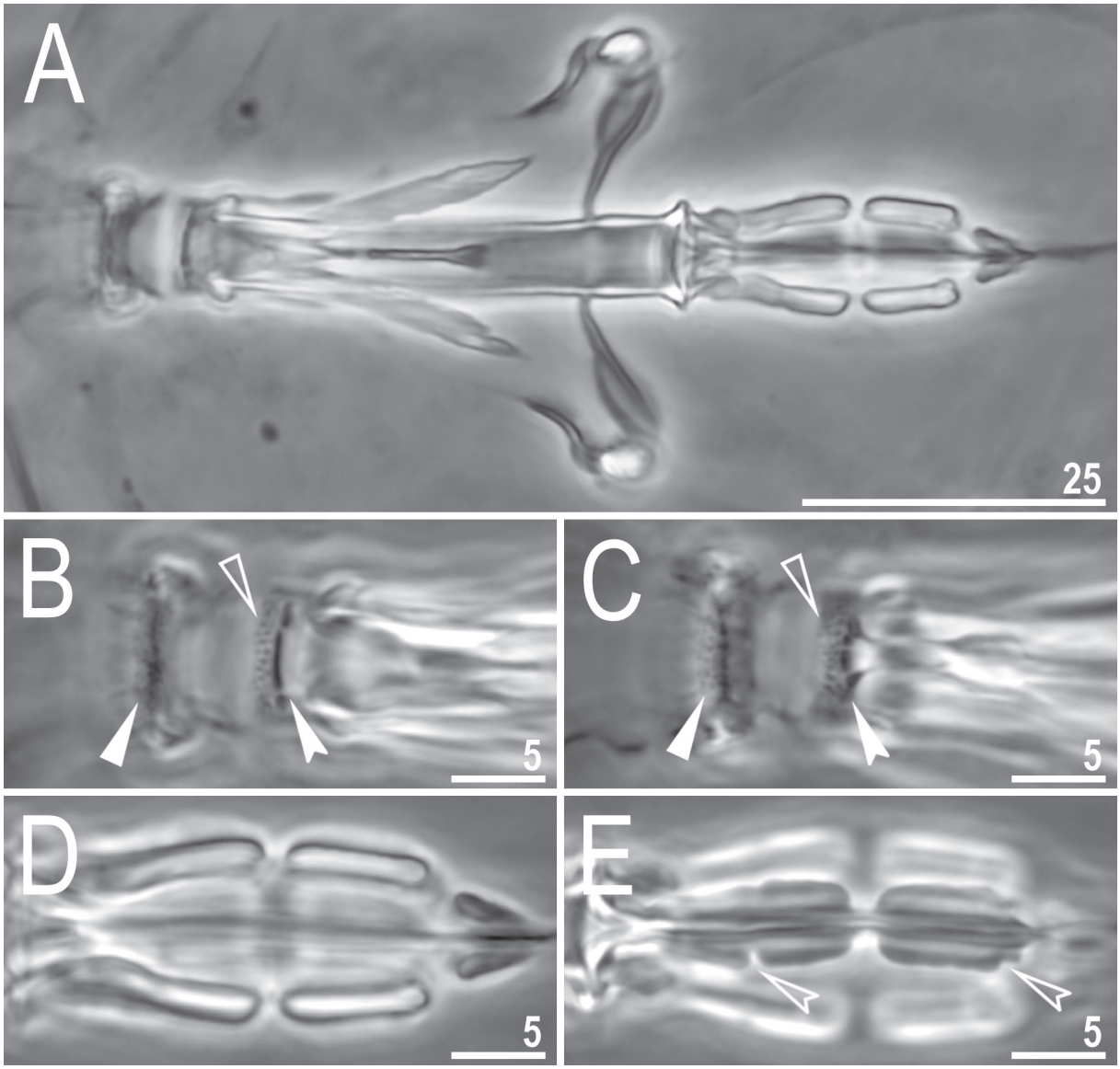

Fig. 17. *Macrobiotus mileri* sp. nov., PCM images of the buccal apparatus (all from holotype, IL.001.11, ISEA PAS, forma aporata). **A**. An entire buccal apparatus. **B**–**C**. The oral cavity armature, dorsal and ventral teeth respectively. **D**–**E**. Placoid morphology, dorsal and ventral placoids, respectively. The filled flat arrowheads indicate the first band of teeth, the empty flat arrowheads indicate the second band of teeth, the filled indented arrowheads indicate the third band of teeth, and the empty indented arrowheads indicate central and subterminal constrictions in the first and second macroplacoid, respectively. Scale bars in μm.

Table 4. Measurements [in µm] and *pt* values of selected morphological structures of animals of *Macrobiotus mileri* sp. nov.; specimens mounted in Hoyer's medium; N: number of specimen/structures measured; range: refers to the smallest and the largest structure among all measured specimens; SD: standard deviation.

Character	N	Range		Mean		SD		Holotype	
		µm	*pt*	µm	*pt*	µm	*pt*	µm	*pt*
Body length	20	326–523	*1101–1392*	449	*1251*	54	*71*	488	*1217*
Buccal tube									
Buccal tube length	20	29.5–40.8	–	35.8	–	3.4	–	40.1	–
Stylet support insertion point	20	23.3–32.8	*78.9–81.3*	28.5	*79.7*	2.7	*0.6*	32.0	*79.8*
Buccal tube external width	20	4.3–6.7	*14.4–17.3*	5.8	*16.1*	0.7	*0.8*	6.4	*16.0*
Buccal tube internal width	20	3.0–5.2	*9.7–13.1*	4.2	*11.7*	0.6	*0.9*	5.1	*12.7*
Ventral lamina length	19	17.2–24.2	*53.5–60.4*	20.8	*57.6*	1.9	*1.9*	23.4	*58.4*
Placoid lengths									
Macroplacoid 1	20	7.0–12.2	*23.5–30.2*	9.7	*26.9*	1.6	*2.2*	12.1	*30.2*
Macroplacoid 2	20	4.6–7.5	*12.3–20.8*	6.1	*17.1*	0.9	*1.8*	7.3	*18.2*
Microplacoid	20	2.5–4.9	*8.4–13.3*	3.8	*10.5*	0.6	*1.2*	4.1	*10.2*
Macroplacoid row	20	12.9–20.9	*42.7–52.2*	17.2	*47.9*	2.4	*2.9*	20.9	*52.1*
Placoid row	20	16.3–26.6	*54.3–67.7*	22.1	*61.6*	3.0	*3.8*	26.6	*66.3*
Claw I heights									
External primary branch	18	7.2–12.9	*24.4–34.1*	10.5	*29.0*	1.4	*2.3*	11.0	*27.4*
External secondary branch	11	7.1–10.0	*22.8–30.2*	9.1	*25.2*	0.9	*2.1*	10.0	*24.9*
Internal primary branch	18	7.1–11.5	*24.1–31.1*	9.9	*27.3*	1.1	*1.6*	10.7	*26.7*
Internal secondary branch	12	7.0–10.1	*21.4–27.1*	9.0	*24.3*	1.0	*1.6*	9.1	*22.7*
Claw II heights									
External primary branch	18	8.3–13.0	*26.8–38.1*	11.3	*31.3*	1.5	*2.8*	12.5	*31.2*
External secondary branch	10	7.7–12.0	*23.1–32.3*	10.0	*27.2*	1.4	*3.0*	10.9	*27.2*
Internal primary branch	15	7.4–11.0	*24.8–29.5*	9.7	*26.9*	1.1	*1.4*	10.1	*25.2*
Internal secondary branch	10	6.2–10.2	*20.8–27.3*	8.9	*23.9*	1.2	*2.1*	9.8	*24.4*
Claw III heights									
External primary branch	16	8.1–12.9	*27.2–34.6*	11.2	*30.9*	1.2	*1.9*	12.3	*30.7*
External secondary branch	11	7.5–11.9	*22.8–31.9*	10.0	*27.1*	1.3	*2.6*	10.6	*26.4*
Internal primary branch	13	7.3–11.2	*24.5–30.0*	9.9	*27.2*	1.2	*1.5*	10.8	*26.9*
Internal secondary branch	10	6.0–10.4	*20.1–27.9*	9.0	*24.0*	1.5	*2.6*	10.0	*24.9*
Claw IV heights									
Anterior primary branch	18	7.4–12.1	*24.8–31.4*	10.4	*28.8*	1.4	*2.0*	12.1	*30.2*
Anterior secondary branch	13	8.2–10.7	*20.1–27.8*	9.1	*24.5*	0.7	*2.1*	10.7	*26.7*
Posterior primary branch	20	8.2–13.1	*23.8–38.4*	11.1	*31.1*	1.5	*3.2*	12.2	*30.4*
Posterior secondary branch	9	6.9–10.9	*20.8–27.9*	9.3	*25.0*	1.3	*2.2*	?	*?*

Eggs

Laid freely, white, spherical and ornamented (Figs 19A–E, 20A–F). The surface between processes is of intermediate state between the *maculatus* and the *persimilis* types, that is, the surface is solid and wrinkled with very small pores, which are present mainly around the bases of the egg processes, and only some are sparse and irregularly distributed in the egg surface between processes (Figs 19A–C, 20C–F). These pores are visible under PCM, but better visible under SEM (0.1–0.3) µm in diameter; Figs19A–C,

20C–F). The processes are not in the shape of inverted goblets with mostly sigmoidal (sometimes concave) conical trunks and weakly defined convex terminal discs with smooth edges (Figs 19A–C, 20C–F). Very faint annulations are visible on the process trunk, especially on the distal portion of the process (character visible only under SEM; Fig. 20D). A crown of gently marked thickenings is visible around the bases of the processes as darker dots under PCM (Fig. 19A–C) and as thicker wrinkles at the processes bases under SEM (Fig. 20D–F). In some processes under SEM the terminal discs have pores in the center (Fig. 20D–F), which under PCM are visible as large light-refracting dot in the disc center (Fig. 19A–C). However, it cannot be excluded that the actual pores in the terminal discs are preparation artefacts, while light refracting dots visible under PCM are caused by thinner chorion layers in this place. The measurements and statistics of eggs are given in Table 5.

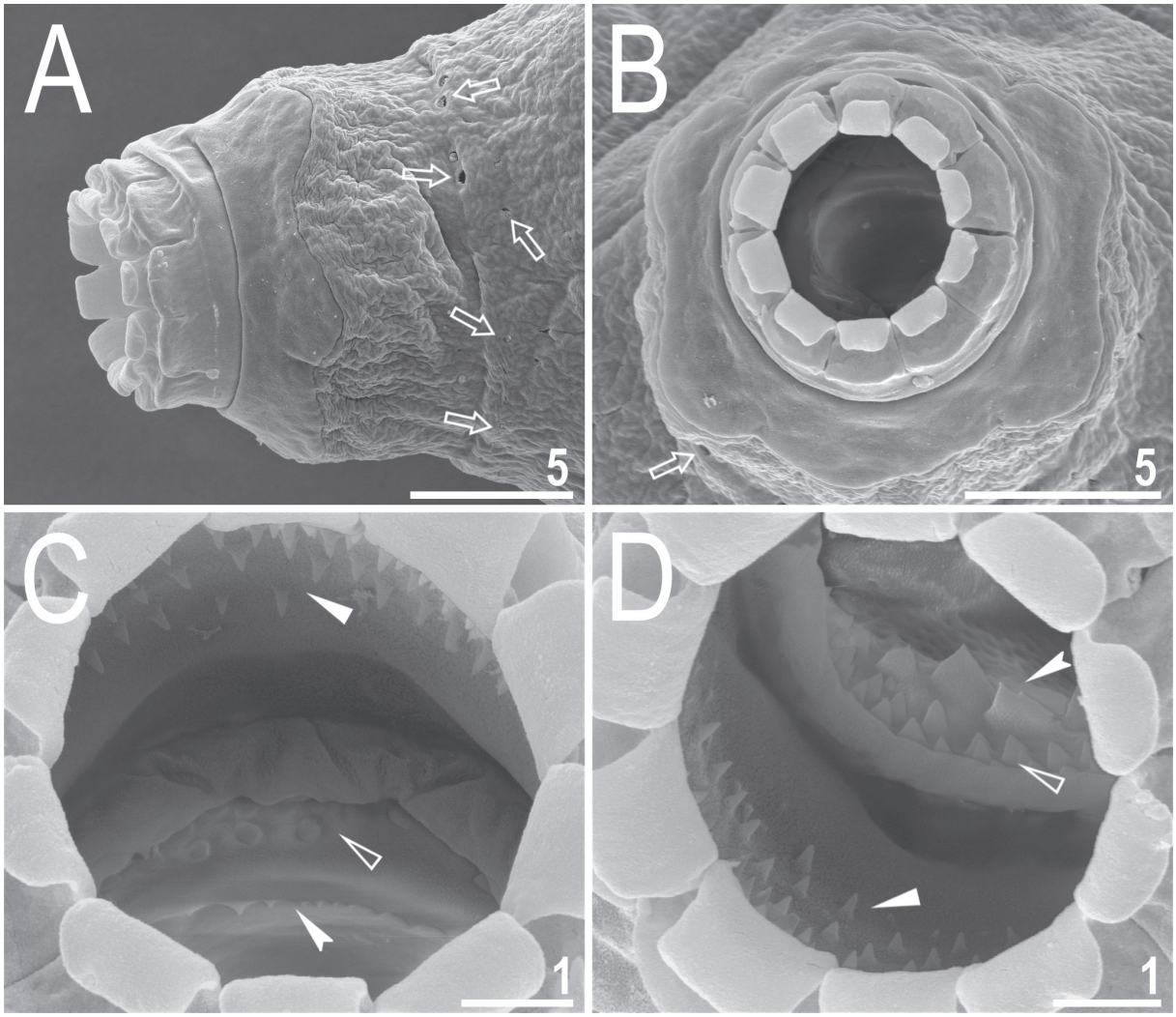

Fig. 18. *Macrobiotus mileri* sp. nov., mouth opening and the oral cavity armature seen under SEM (paratypes, ISEA PAS). **A–B**. The mouth opening of a single paratype visible from lateral and frontal view respectively. **C**–**D**. The oral cavity armature of a single paratype seen under SEM from different angles, dorsal (C) and ventral (D) view, respectively. Empty arrows indicate cuticular pores, filled flat arrowheads indicate the first band of tenth, empty flat arrowheads indicate the second band of teeth, and filled indented arrowheads indicate the third band of teeth. Scale bars in μm.

Table 5. Measurements [in µm] of the eggs of *Macrobiotus mileri* sp. nov.; eggs mounted in Hoyer's medium; process base/height ratio is expressed as percentage; N: number of eggs/structures measured; range: refers to the smallest and the largest structure among all measured specimens; SD: standard deviation.

Character	N	Range	Mean	SD
Egg bare diameter	7	76.5– 92.6	82.5	6.2
Egg full diameter	7	93.0– 107.6	98.2	6.3
Process height	21	6.2– 8.7	7.6	0.8
Process base width	21	7.3– 10.3	8.5	0.6
Process base/height ratio	21	93%– 140%	113%	14%
Terminal disc width	21	2.2– 4.2	3.2	0.4
Inter-process distance	21	1.2– 3.3	2.4	0.5
Number of processes on the egg circumference	7	23– 25	24.0	0.8

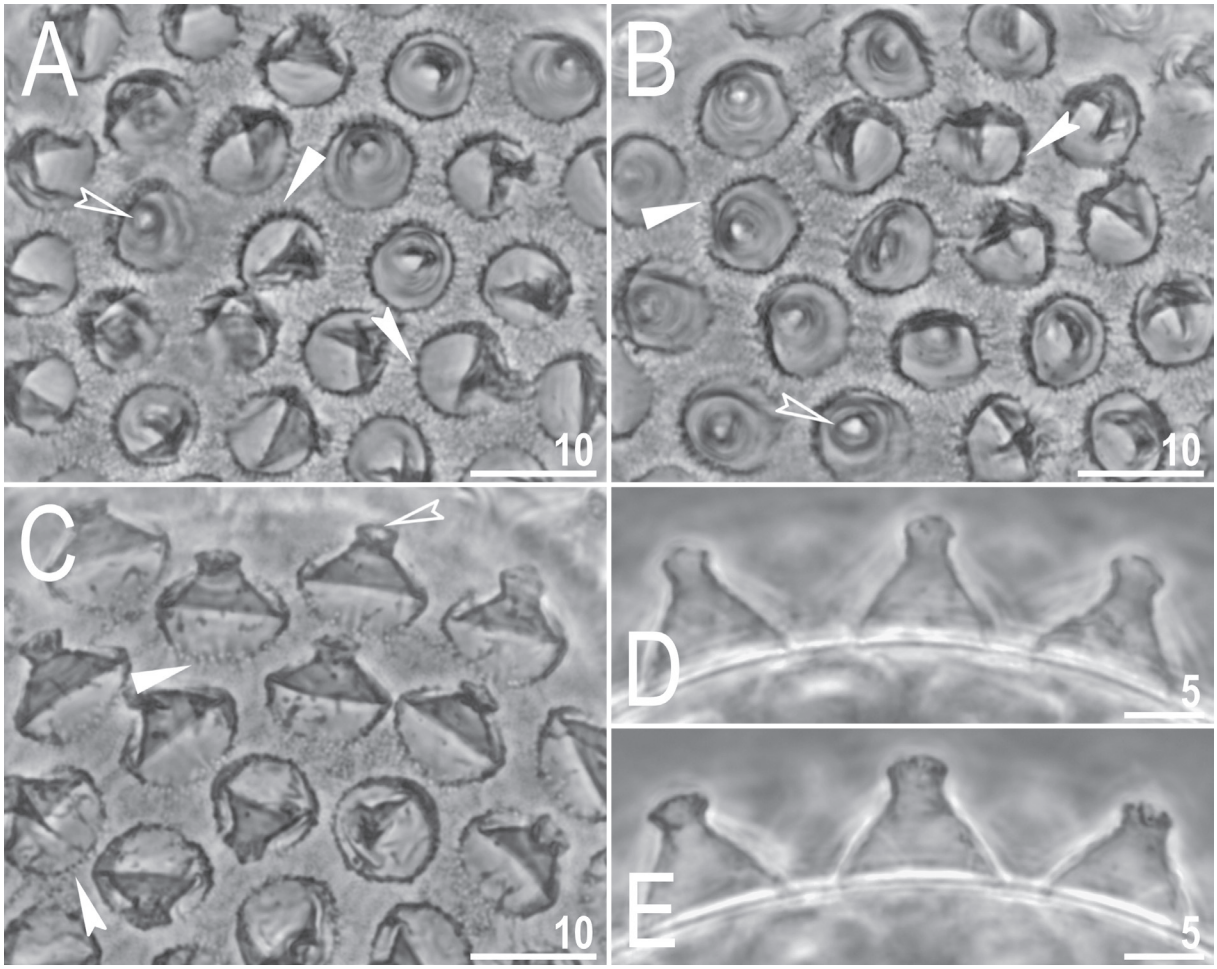

Fig. 19. *Macrobiotus mileri* sp. nov., PCM images of the eggs under ×1000 magnification (ISEA PAS). **A–C**. Egg surface. **D**–**E**. Midsections of egg processes. Empty indented arrowheads indicate pores / light-refracting dots in the center of the terminal discs, filled flat arrowheads indicate small pores around bases of the egg processes, filled indented arrowheads indicate dark thickenings around bases of the egg processes. Scale bars in µm.

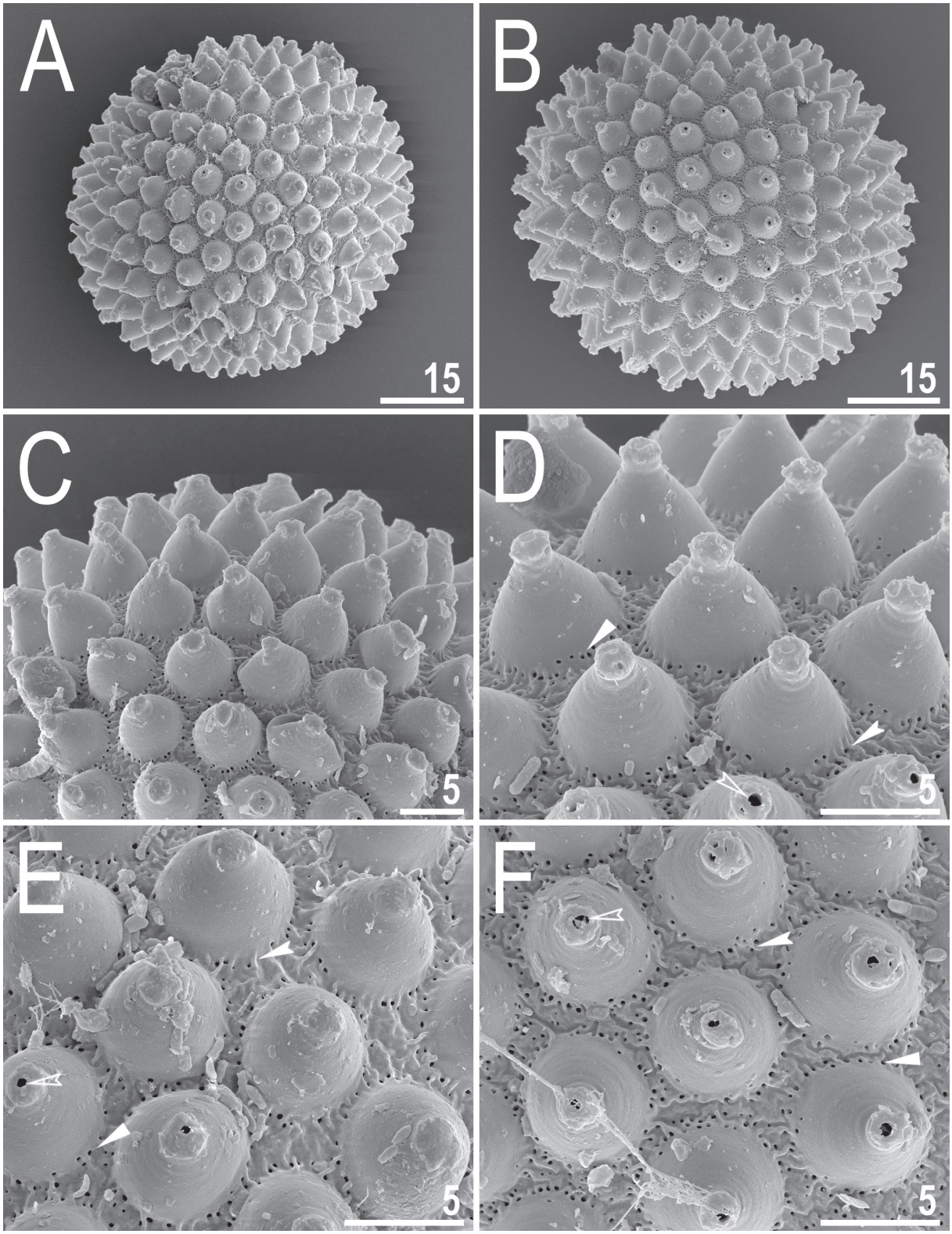

Fig. 20. *Macrobiotus mileri* sp. nov., SEM images of eggs (ISEA PAS). **A**–**B**. Entire egg. **C**–**F**. Details of egg processes and the surface between them. Empty indented arrowheads indicate pores in center of terminal discs, filled flat arrowheads indicate small pores around bases of egg processes, filled indented arrowheads indicate thickenings around bases of egg processes. Scale bars in μm.

Reproduction

The type population of *M. mileri* sp. nov. is dioecious. Both males with testes filled with sperm and females with ovaries containing oocytes were observed in specimens freshly mounted in Hoyer's medium in both specimens ascribed to each of the two morphological forms.

Differential diagnosis

By having (i) three bands of teeth in the oral cavity armature that are well visible under light microscope, (ii) the entire body cuticle covered by granulation (sometimes visible only under SEM), the new species is the most similar to five other taxa of *Macrobiotus*, namely *Macrobiotus joannae* Pilato & Binda, 1983 reported from its type locality in Australia (Pilato & Binda 1983), and several uncertain localities in central, eastern, and south-eastern Russia (Biserov 1990) and from Italy (Bertolani *et al.* 2014), *Macrobiotus hannae* Nowak & Stec, 2018 known only from its type locality in Poland (Nowak & Stec 2018), *Macrobiotus punctillus* Pilato, Binda & Azzaro, 1990 known only from its type locality in Chile (Pilato *et al.* 1990), *Macrobiotus rebecchii* Stec, 2022 known only from its type locality in Kyrgyzstan (Stec 2022b) and *M. ovovittatus* sp. nov. described above. However, it can be easily distinguished from all of them by having different pores arrangements on the body cuticles (two forms: porata with pores arranged in five distinct patches; and aporata with singular, small, almost undetectable pores vs typical, more or less evenly distributed cuticular pores in the other species) and a different morphology of the terminal discs (weakly defined convex terminal discs with smooth edges in the new species vs cog-shaped terminal discs, with a concave central area and 10–18 distinct teeth in the other species).

Phylogenetic and delimitation results

Both phylogenetic analyses resulted in trees of similar topology, and most of the nodes well and moderately supported, in which three distinct monophyletic *Macrobiotus* lineages (*Macrobiotus* clades A, B, and C) were confidently recovered (Fig. 21, Supp. file 3). The analyses confirmed also monophyly for the *M. ariekammensis*, *M. pallarii*, and *M. pseudohufelandi* complexes (Fig. 21). At first, it seems that the *Macrobiotus polonicus-persimilis* complex as defined by Bertolani *et al.* (2023) has also been recovered to be monophyletic. However, the position of *M.* cf. *polonicus* 1 and 2 from Sweden (Vecchi & Stec 2021), whose morphology also fits this definition, makes this species complex paraphyletic. Also, the *M. polonicus* species complex as defined by Stec *et al.* (2021a) or the *M. persimilis* morpho-group as defined by Bertolani *et al.* (2023) is paraphyletic, since *M.* cf. *polonicus* from Sweden and *Macrobiotus annewintersae* Vecchi & Stec, 2021 cluster together with species of the *M. pallarii* complex. *Macrobiotus mileri* sp. nov. belongs to the *Macrobiotus* clade B staying in sister relationship with the clade containing *Macrobiotus caelestis* Coughlan, Michalczyk & Stec, 2019 and nominal taxa of the *M. polonicus-persimilis* complex (Fig. 21). The second new species, *M. ovovittatus* sp. nov., belongs to the *Macrobiotus* clade A, as the closest relative of *Macrobiotus hupingensis* Yuan, Wang, Liu, Liu & Li, 2022 and together they cluster with *Macrobiotus birendrai* Kayastha, Roszkowska, Mioduchowska, Gawlak & Kaczmarek, 2021, *M. hannae* and *M. rebecchii* (Fig. 21). Importantly, *M. hupingensis* is a species of the *M. pallarii* complex, but the DNA sequences associated with this description belong to different unspecified *Macrobiotus* and the authors are working on correcting this mistake (Z. Yuan, Shaanxi Normal University, pers. com.). Therefore, the species name is given within quotation marks in the phylogenetic tree (Fig. 21).

The delimitation results of both ASAP analyses were congruent (Supp. file 4). The number of delimited species from the COI data set representing Macrobiotidae superclade I, and for the data set comprising only taxa of *Macrobiotus*, were 73 and 47, respectively. The number of taxa of *Macrobiotus* delimited in the larger data set was the same as for the smaller data set (47; Supp. file 4). Two new species described in this study have always been distinguished as two distinct entities (Supp. file 4). Both morphological forms within *M. mileri* sp. nov. have also been recognized as a single species (Supp. file 4). Interestingly,

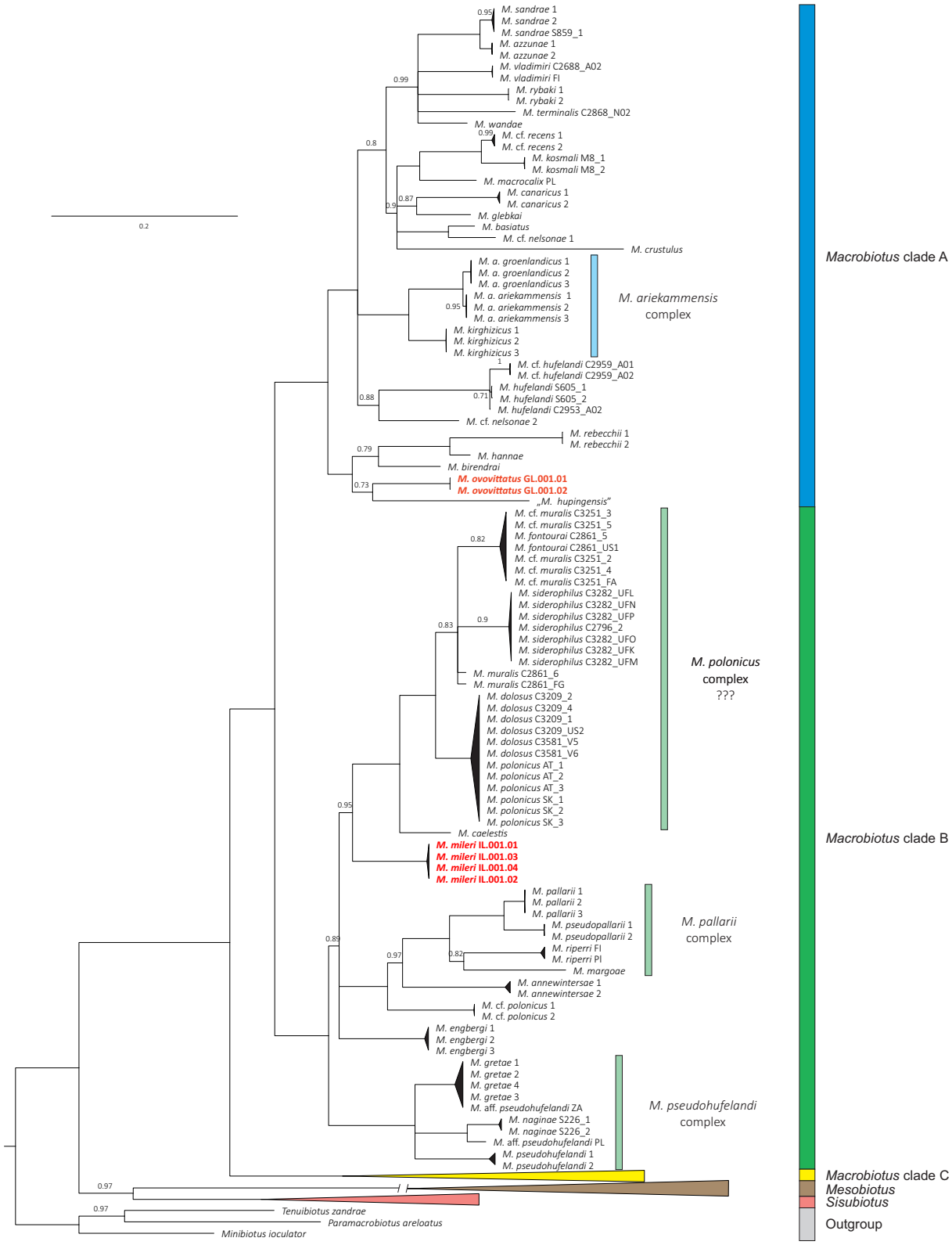

Fig. 21. Bayesian phylogenetic reconstruction of Superclade I of the family Macrobiotidae. Values at nodes are BI posterior probability supports, nodes with support < 0.70 were collapsed whereas nodes with maximum support values (1.00) are not shown. Newly sequenced taxa are bolded and marked with red font. The scale bar represents substitutions per position.

there were several cases where taxa that were potentially thought as being distinct have been lumped together into singular putative species. These were: (i) *Macrobiotus sandrae* Bertolani & Rebecchi, 1993 and *Macrobiotus azzunae* Ben Marnissi, Cesari, Rebecchi & Bertolani, 2021, (see Ben Marnissi *et al.* 2021), (ii) *Macrobiotus hufelandi* Schultze, 1834 and *M.* cf. *hufelandi* (see Bertolani *et al.* 2011), (iii) *Macrobiotus fontourai* Bertolani, Cesari, Giovannini, Rebecchi, Guidetti, Kaczmarek & Pilato, 2022 and *M.* cf. *muralis* (see Bertolani *et al.* 2023), (iv) *Macrobiotus kosmali* Kayastha, Mioduchowska, Gawlak, Sługocki, Gonçalves Silva & Kaczmarek, 2023 and *M.* cf. *recens* (see Kayastha *et al.* 2023).

Discussion

Macrobiotus ovovitattus sp. nov.

The phylogenetic analysis recovered a clade that, together with *M. ovovittatus* sp. nov., includes *M. hannae*, *M. rebecchii*, *M. birendrai,* and "*M. hupingensis*". The latter species, was described as belonging to the *Macrobiotus pallarii* group by Yuan *et al.* (2022); however, it is most likely that the published sequences belong to a different species. Yuan *et al.* (2022) only compared the COI sequences to other species of the *Macrobiotus pallarii* group, thus making it impossible to detect the mistake. Two other species in the clade, *M. hannae* and *M. rebecchii*, have been confirmed to be hermaphroditic (Nowak & Stec 2018; Stec 2022a). The reproductive mode of *M. birendrai* and "*M. hupingensis*" is unfortunately unknown (Kayastha *et al.* 2021; Yuan *et al.* 2022). However, it should be noted that in the original description of *M. birendrai*, more than 60 animals were analysed without finding any evidence of the presence of males. Similarly, also for *M. ovovittatus* sp. nov., males or sperm have not been observed despite a careful examination of specimens freshly mounted in Hoyer's medium and specimens stained with orcein. Moreover, it is also important to point out that all these nominal taxa are morphologically very similar to two other species, *M. punctillus* and *M. joannae*, of which the latter is likewise confirmed to be hermaphroditic. Morphological similarity between the abovementioned species can also be observed in the egg chorion, especially when comparing the SEM data (Nowak & Stec 2018; Stec 2022b; Kayastha *et al.* 2021; this study). Taking all these fragmentary information into consideration, it might be hypothesized that in the recovered clade hermaphroditism is common (opposed to its overall rarity in tardigrades).

Macrobiotus mileri sp. nov.

The second newly described species, *M. mileri* sp. nov., is found in the same clade as the species of the *M. persimilis* morphogroup sensu Bertolani *et al.* (2023), species in this morphogroup exhibit a solid egg surface without reticulation or pores. However, this new species can be considered as an exception due to three main peculiarities. The first is that the animals have different alternative morphological forms (one with big, specifically arranged cuticular pores and one with singular, rare, almost impossible to notice and small pores distributed randomly on the body cuticle). Such different morphologies within one species might be ascribed to phenomena already noted in tardigrades, like cyclomorphosis (e.g., Kristensen 1982; Møbjerg *et al.* 2007) or ontogenetic changes (e.g., Surmacz *et al.* 2019, 2020). However, since cyclomorphosis is a seasonal cyclic change in morphology (thus linked to specific temporal windows), a more probable explanation for these different forms (found together at the same time) in *M. mileri* sp. nov. is an ontogenetic change. In this case, different morphologies are exhibited by different developmental stages of an animal, hence a greater possibility of finding different forms within the same population at the same time. Although such drastically disjunct animal morphologies regarding cuticular pores have not been reported so far for any member of the family Macrobiotidae, one example is known within the superfamily Macrobiotoidea. Specifically, in the genus *Richtersius* Pilato & Binda, 1989 only the first instar animals (hatchlings) possess cuticular pores (Guidetti *et al.* 2016; Kayastha *et al.* 2020a; Stec *et al.* 2020b; Pogwizd & Stec 2022; Kiosya & Stec 2022). The second peculiarity can be noticed in the egg chorion morphology. The fact that the new species, have reduced terminal discs but cluster together with taxa having well-developed terminal discs in egg processes once

again underlines a large evolutionary plasticity regarding morphological evolution of egg characters (Guidetti *et al.* 2013; Stec *et al.* 2016b, 2021a). Although the new species is related to taxa exhibiting so-called *persimilis* morphology, the reduced terminal discs and small pores in the egg surface between the processes prevent its inclusion in the *persimilis* morphogroup sensu Bertolani *et al.* (2023). This further stresses that the morphogroups do not reflect phylogenetic relatedness, thus no formal taxonomic rank or nomenclatural acts should be attributed to them. The third peculiarity of the new species is the presence of a garter-shaped structure (Massa *et al.* 2021) on legs I–III, which was previously suggested to be an adaptation to soil and sandy habitats characteristic of the *M. pseudohufelandi* complex, previously known as *Xerobiotus* Bertolani & Biserov, 1996 (Massa *et al.* 2021; Stec *et al.* 2021a, 2022).

Macrobiotus mileri sp. nov., in the debate on the *Xerobiotus/Macrobiotus pseudohufelandi* complex

The presence of a garter-shaped structure in *Macrobiotus mileri* sp. nov., a species not related to the *Xerobiotus/M. pseudohufelandi* complex, invalidates this trait as diagnostic synapomorphy of the previously suppressed genus *Xerobiotus*. A similar structure was also identified in *Eremobiotus* by Gąsiorek *et al.* (2019); however, given the evolutionary distance between *Eremobiotus* and Macrobiotidae, there is the possibility that those structure are not homologous, but evolved independently as an adaptation to the same habitat. Contrarily to *Eremobiotus*, *M. mileri* sp. nov. is instead a closer relative of the *Xerobiotus/M. pseudohufelandi* complex, supporting the homology of this structure and dispelling its usefulness as a diagnostic synapomorphic trait for *Xerobiotus*. Bertolani *et al.* (2023) proposed to reinstate the genus *Xerobiotus* due to its clear morphological synapomorphies, keeping at the same time the genus *Macrobiotus* paraphyletic, and argued that "confirmation through synapomorphies must be sought before erecting and/or suppressing taxa". However, the identification of one putative synapomorphy of *Xerobiotus* in another species of *Macrobiotus* erodes the set of synapomorphies supporting *Xerobiotus*. Recently, a paper proposing the resurrection of *Xerobiotus* has been published (Vincenzi *et al.* 2023). The authors found the phylogenetic position of *Xerobiotus* to be the same as in previous studies (which used the phylogenetic position as an argument for its suppression), but decided to reinstate the taxon based on its morphological distinctiveness. Surprisingly, their phylogenetic analyses seem to recover *Xerobiotus* as not monophyletic, since the newly sequenced *Pseudohexapodibius degenerans* (Biserov, 1990) is placed within it. On the other hand, genetic species delimitation performed in this new study suggested *P. degenerans* to be a synonym of one *Xerobiotus* species analysed therein. This indicates that distinguishing *Pseudohexapodibius* Bertolani & Biserov, 1996 by its extreme hind leg and claw reduction does not reflect the phylogenetic reconstruction. Such results support the suppression of *Pseudohexapodibius*, but this action has not been undertaken (Vincenzi *et al.* 2023). While the genetic data from this new publication were not available at the time, hindering reanalyses, it is unlikely that the outcome of this study would have differed significantly. The monophyly and phylogenetic position of the taxa within the *Macrobiotus* clade B (including the *Xerobiotus/M. pseudohufelandi* complex and *M. mileri* sp. nov.) have remained consistent across all published studies on this subject (Massa *et al.* 2021; Stec *et al.* 2021a, 2022; Vincenzi *et al.* 2023).

The approach, where a young evolutionary lineage is placed within a clade that exhibits a more conservative form, will disrupt the unity of the larger group. To ensure that the taxonomy accurately reflects the evolutionary history of tardigrades, it is crucial to avoid disrupting the unity of higher systematic ranks as already extensively explained in recent revisions (Stec *et al.* 2021a, 2022). Therefore, it should be advised that instead of hastily establishing or mantaining genera based on limited supporting evidence, it would be more appropriate to identify species complexes that emphasize the morphological and evolutionary characteristics of these lineages. Importantly, species complexes carry no nomenclatural implications and do not affect the hierarchical status of higher systematic ranks. Nonetheless, they contribute significantly to a better organization and navigation within the field of systematics. This approach aligns with the modern goal of recognizing monophyletic groups, and I

believe that subdividing the diverse yet monophyletic *Macrobiotus* into species complexes and morpho-groups provides a more flexible perspective. As such, it should be considered a preferable standpoint for future systematic and phylogenetic studies within Macrobiotidae.

Conclusions

Comprehensive analyses that incorporate multiple biological dimensions, including morphology, behavior, molecular characteristics, and genetic variation, are now commonly employed in species delineation (Goldstein & DeSalle 2011; Vinarski 2020). These analyses generally result in coherent and stable taxonomic units that consider evolutionary histories. Thanks to comprehensive taxon sampling and combined comparative analyses of morphological and genetic data, I was able to (i) formally describe two new tardigrade species and (ii) provide an updated perspective on the *Macrobiotus* phylogeny. The results emphasize that the morphological diagnostic characters traditionally and commonly used to differentiate and identify species within this tardigrade group appear to be considerably flexible, making it challenging to recognize monophyletic entities. In addition, I discuss how one of the newly described species provides insights into the debate about the reinstatement of the genus *Xerobiotus*.

Acknowledgments

I am particularly grateful to Krzysztof Miler (Institute of Systematics and Evolution of Animals, Polish Academy of Sciences), Piotr Łukasik, and Michał Kolasa (both from Jagiellonian University) for generously providing the samples that enabled me to conduct this study. The collections were made possible through the support of the Polish National Agency for Academic Exchange, with the Bekker scholarship awarded to KM, and the International Network for Terrestrial Research and Monitoring in the Arctic (INTERACT) Transnational Access grant in 2021 awarded to PŁ. I would also like to express my appreciation to Edoardo Massa (University of Modena and Reggio Emilia) for his valuable advice on the naming of the new species, as well as to two anonymous reviewers for their constructive comments and suggestion which improved the manuscript. This study received support from the European Commission's program 'Transnational Access to Major Research Infrastructures' through the SYNTHESYS grant (grant no. DK-TAF-TA4-005 to DS) and from the Institute of Systematics and Evolution of Animals, Polish Academy of Sciences.

References

Astrin J.J. & Stüben P.E. 2008. Phylogeny in cryptic weevils: molecules, morphology and new genera of western Palaearctic Cryptorhynchinae (Coleoptera: Curculionidae). *Invertebrate Systematics* 22: 503–522. https://doi.org/10.1071/IS07057

Ben Marnissi J., Cesari M., Rebecchi L. & Bertolani R. 2021. Integrative description of a new Tunisian tardigrade species, *Macrobiotus azzunae* sp. nov. (Eutardigrada, Macrobiotidae, *hufelandi* group). *European Journal of Taxonomy* 758: 122–146. https://doi.org/10.5852/ejt.2021.758.1429

Bertolani R. 1971. Rapporto-sessi e dimorfismo sessuale in *Macrobiotus* (Tardigrada). *Atti della Accademia Nazionale dei Lincei* 50: 377–382.

Bertolani R., Rebecchi L., Giovannini I. & Cesari M. 2011. DNA barcoding and integrative taxonomy of *Macrobiotus hufelandi* C.A.S. Schultze 1834, the first tardigrade species to be described, and some related species. *Zootaxa* 2997: 19–36. https://doi.org/10.11646/zootaxa.2997.1.2

Bertolani R., Guidetti R., Marchioro T., Altiero T., Rebecchi L. & Cesari M. 2014. Phylogeny of Eutardigrada: New molecular data and their morphological support lead to the identification of new evolutionary lineages. *Molecular Phylogenetics and Evolution* 76: 110–126. https://doi.org/10.1016/j.ympev.2014.03.006

Bertolani R., Cesari M., Giovannini I., Rebecchi L., Guidetti R., Kaczmarek Ł. & Pilato G. 2023. The *Macrobiotus persimilis-polonicus* complex (Eutardigrada, Macrobiotidae), another example of problematic species identification, with the description of four new species. *Organisms Diversity & Evolution* 23: 329–368. https://doi.org/10.1007/s13127-022-00599-z

Biserov V.I. 1990. On the revision of the genus *Macrobiotus*. The subgenus *Macrobiotus* s. st. is a new systematic status of the *hufelandi* group (Tardigrada, Macrobiotidae). Communication 2. *Zoologicheskij Zhurnal* 69 (12): 38–50.

Casquet J.T., Thebaud C. & Gillespie, R.G. 2012. Chelex without boiling, a rapid and easy technique to obtain stable amplifiable DNA from small amounts of ethanol-stored spiders. *Molecular Ecology Resources* 12: 136–141. https://doi.org/10.1111/j.1755-0998.2011.03073.x

Castresana J. 2000. Selection of conserved blocks from multiple alignments for their use in phylogenetic analysis. *Molecular Biology and Evolution* 17: 540–552. https://doi.org/10.1093/oxfordjournals.molbev.a026334

Cesari M., Giovannini I., Altiero T., Guidetti R., Cornette R., Kikawada T. & Rebecchi L. 2022. Resistance to extreme stresses by a newly discovered Japanese tardigrade species, *Macrobiotus kyoukenus* (Eutardigrada, Macrobiotidae). *Insects* 13: 634. https://doi.org/10.3390/insects13070634

Coughlan K. & Stec D. 2019. Two new species of the *Macrobiotus hufelandi* complex (Tardigrada: Eutardigrada: Macrobiotidae) from Australia and India, with notes on their phylogenetic position. *European Journal of Taxonomy* 573: 1–38. https://doi.org/10.5852/ejt.2019.573

Coughlan K., Michalczyk Ł. & Stec D. 2019. *Macrobiotus caelestis* sp. nov., a new tardigrade species (Macrobiotidae: *hufelandi* group) from the Tien Shan mountains (Kyrgyzstan). *Annales Zoologici* 69 (3): 499–513. https://doi.org/10.3161/00034541ANZ2019.69.3.002

Degma P. & Guidetti R. 2023. *Actual Checklist of Tardigrada Species*. Università di Modena e Reggio Emilia. https://doi.org/10.25431/11380_1178608

Gąsiorek P., Stec D., Morek W. & Michalczyk Ł. 2019. Deceptive conservatism of claws: distinct phyletic lineages concealed within Isohypsibioidea (Eutardigrada) revealed by molecular and morphological evidence. *Contributions to Zoology* 88 (1): 78–132. https://doi.org/10.1163/18759866-20191350

Goldstein P.Z. & DeSalle R. 2011. Integrating DNA barcode data and taxonomic practice: Determination, discovery, and description. *Bioessays* 33: 135–147. https://doi.org/10.1002/bies.201000036

Guidetti R., Peluffo J.R., Rocha A.M., Cesari M. & Moly de Peluffo M.C. 2013. The morphological and molecular analyses of a new South American urban tardigrade offer new insights on the biological meaning of the *Macrobiotus hufelandi* group of species (Tardigrada: Macrobiotidae). *Journal of Natural History* 47 (37–38): 2409–2426. https://doi.org/10.1080/00222933.2013.800610

Guidetti R., Rebecchi L., Bertolani R., Jönsson K.I., Kristensen R.M. & Cesari M. 2016. Morphological and molecular analyses on *Richtersius* (Eutardigrada) diversity reveal its new systematic position and lead to the establishment of a new genus and a new family within Macrobiotoidea. *Zoological Journal of the Linnean Society* 178 (4): 834–845. https://doi.org/10.1111/zoj.12428

Hall T.A. 1999. BioEdit: a user-friendly biological sequence alignment editor and analysis program for Windows 95/98/NT. *Nucleic Acids Symposium Series* 41: 95–98.

Hoang D.T., Chernomor O., von Haeseler A., Minh B.Q. & Vinh L.S. 2018. UFBoot2: improving the ultrafast bootstrap approximation. *Molecular Biology and Evolution* 35: 518–522. https://doi.org/10.1093/molbev/msx281

Itang L.A.M., Stec D., Mapalo M.A., Mirano-Bascos D. & Michalczyk Ł. 2020. An integrative description of *Mesobiotus dilimanensis*, a new tardigrade species from the Philippines (Eutardigrada: Macrobiotidae: *furciger* group). *Raffles Bulletin of Zoology* 68: 19–31.

Kaczmarek Ł. & Michalczyk Ł. 2017. The *Macrobiotus hufelandi* (Tardigrada) group revisited. *Zootaxa* 4363 (1): 101–123. https://doi.org/10.11646/zootaxa.4363.1.4

Kaczmarek Ł., Cytan J., Zawierucha K., Diduszko D. & Michalczyk Ł. 2014. Tardigrades from Peru (South America), with descriptions of three new species of Parachela. *Zootaxa* 3790 (2): 357–379. https://doi.org/10.11646/zootaxa.3790.2.5

Kaczmarek Ł., Zawierucha K., Buda J., Stec D., Gawlak M., Michalczyk Ł. & Roszkowska M. 2018. An integrative redescription of the nominal taxon for the *Mesobiotus harmsworthi* group (Tardigrada: Macrobiotidae) leads to descriptions of two new *Mesobiotus* species from Arctic. *PLoS ONE* 13 (10): e0204756. https://doi.org/10.1371/journal.pone.0204756

Kaczmarek Ł., Bartylak T., Stec D., Kulpa A., Kepel M., Kepel A. & Roszkowska M. 2020. Revisiting the genus *Mesobiotus* Vecchi *et al.*, 2016 (Eutardigrada, Macrobiotidae) – remarks, updated dichotomous key and an integrative description of new species from Madagascar. *Zoologischer Anzeiger* 287: 121–146. https://doi.org/10.1016/j.jcz.2020.05.003

Kaczmarek Ł., Rutkowski T., Zacharyasiewicz M., Surmacki A., Osiejuk T.S. & Hayastha P. 2023. New species of Macrobiotidae (Eutardigrada) from Cameroon (Africa), characteristics of *Macrobiotus* morpho-groups and a key to the *nelsonae* group. *Annales Zoologici* 73: 1–15. https://doi.org/10.3161/00034541ANZ2023.73.1.001

Kalyaanamoorthy S., Minh B.Q., Wong T.K.F., von Haeseler A. & Jermiin L.S. 2017. ModelFinder: fast model selection for accurate phylogenetic estimates. *Nature Methods* 14: 587–589. https://doi.org/10.1038/nmeth.4285

Katoh K. & Toh H. 2008. Recent developments in the MAFFT multiple sequence alignment program. *Briefings in Bioinformatics* 9: 286–298. https://doi.org/10.1093/bib/bbn013

Katoh K., Misawa K., Kuma K. & Miyata T. 2002. MAFFT: a novel method for rapid multiple sequence alignment based on fast Fourier transform. *Nucleic Acids Research* 30: 3059–3066. https://doi.org/10.1093/nar/gkf436

Kayastha P., Berdi D., Mioduchowska M., Gawlak M., Łukasiewicz A., Gołdyn B. & Kaczmarek Ł. 2020a. Some tardigrades from Nepal (Asia) with integrative description of *Macrobiotus wandae* sp. nov. (Macrobiotidae: *hufelandi* group). *Annales Zoologici* 70 (1): 121–142. https://doi.org/10.3161/00034541ANZ2020.70.1.007

Kayastha P., Berdi D., Mioduchowska M., Gawlak M., Łukasiewicz A., Gołdyn B., Jędrzejewski S. & Kaczmarek Ł. 2020b. Description and molecular characterization of *Richtersius ziemowiti* sp. nov. (Richtersiidae) from Nepal (Asia) with evidence of heterozygous point mutation events in the 28S rRNA. *Annales Zoologici* 70 (3): 381–396. https://doi.org/10.3161/00034541ANZ2020.70.3.010

Kayastha P., Roszkowska M., Mioduchowska M., Gawlak M. & Kaczmarek Ł. 2021. Integrative descriptions of two new tardigrade species along with the new record of *Mesobiotus skorackii* Kaczmarek *et al.*, 2018 from Canada. *Diversity* 13: 394. https://doi.org/10.3390/d13080394

Kayastha P., Mioduchowska M. Gawlak M., Sługocki Ł., Gonçalves Silva A.J.J. & Kaczmarek Ł. 2023. Integrative description of *Macrobiotus kosmali* sp. nov. (*hufelandi* group) from the Island of Madeira (Portugal). *The European Zoological Journal* 90 (1): 126–138. https://doi.org/10.1080/24750263.2022.2163312

Kiosya Y. & Stec D. 2022. New species of the genus *Richtersius* Pilato & Binda, 1989 (Tardigrada: Eutardigrada: Richtersiusidae) from Uzbekistan. *Folia Biologica (Kraków)* 70 (4): 141–150. https://doi.org/10.3409/fb_70-4.18

Kiosya Y., Pogwizd J., Matsko Y., Vecchi M. & Stec D. 2021. Phylogenetic position of two *Macrobiotus* species with a revisional note on *Macrobiotus sottilei* Pilato, Kiosya, Lisi & Sabella, 2012 (Tardigrada: Eutardigrada: Macrobiotidae). *Zootaxa* 4933 (1): 113–135. https://doi.org/10.11646/zootaxa.4933.1.5

Kristensen R.M. 1982. The first record of cyclomorphosis in Tardigrada based on a new genus and species from arctic meiobenthos. *Zeitschrift fur Zoologische Systematik und Evolution Forschung* 20: 249–270. https://doi.org/10.1111/j.1439-0469.1983.tb00552.x

Kuzdrowska K.A., Mioduchowska M., Gawlak M., Bartylak T., Kepel A., Kepel M. & Kaczmarek Ł. 2021. Integrative description of *Macrobiotus porifini* sp. nov. (Macrobiotidae) from Madagascar and its phylogenetic position within the *hufelandi* group. *The European Zoological Journal* 88 (1): 375–389. https://doi.org/10.1080/24750263.2021.1883752

Lanfear R., Frandsen P.B., Wright A.M., Senfeld T. & Calcott B. 2016. PartitionFinder 2: new methods for selecting partitioned models of evolution for molecular and morphological phylogenetic analyses. *Molecular Biology and Evolution* 34: 772–773. https://doi.org/10.1093/molbev/msw260

Mapalo M., Stec D., Mirano-Bascos D.M. & Michalczyk Ł. 2016. *Mesobiotus philippinicus* sp. nov., the first limnoterrestrial tardigrade from the Philippines. *Zootaxa* 4126 (3): 411–426. https://doi.org/10.11646/zootaxa.4126.3.6

Mapalo M., Stec D., Mirano-Bascos D. & Michalczyk Ł. 2017. An integrative description of a limnoterrestrial tardigrade from the Philippines, *Mesobiotus insanis*, new species (Eutardigrada: Macrobiotidae: *harmsworthi* group). *Raffles Bulletin of Zoology* 65: 440–454.

Marley N.J., McInnes S.J. & Sands C.J. 2011. Phylum Tardigrada: A re-evaluation of the Parachela. *Zootaxa* 2819: 51–64. https://doi.org/10.11646/zootaxa.2819.1.2

Massa E., Guidetti R., Cesari M., Rebecchi L. & Jönsson K.I. 2021. Tardigrades of Kristianstads Vattenrike Biosphere Reserve with description of four new species from Sweden. *Scientific Reports* 11: 4861. https://doi.org/10.1038/s41598-021-83627-w

Michalczyk Ł. & Kaczmarek Ł. 2013. The Tardigrada Register: a comprehensive online data repository for tardigrade taxonomy. *Journal of Limnology* 72 (S1): 175–181. https://doi.org/10.4081/jlimnol.2013.s1.e22

Mironov S.V., Dabert J. & Dabert M. 2012. A new feather mite species of the genus *Proctophyllodes* Robin, 1877 (Astigmata: Proctophyllodidae) from the Long-tailed Tit *Aegithalos caudatus* (Passeriformes: Aegithalidae): morphological description with DNA barcode data. *Zootaxa* 3253: 54–61. https://doi.org/10.11646/zootaxa.3253.1.2

Møbjerg N., Jørgensen A., Eibye-Jacobsen J., Agerlin Halberg K., Persson D. & Kristensen R.M. 2007. New records on cyclomorphosis in the marine eutardigrade *Halobiotus crispae* (Eutardigrada: Hypsibiidae). *Journal of Limnology* 66 (Suppl. 1): 132–140. https://doi.org/10.4081/jlimnol.2007.s1.132

Morek W., Stec D., Gąsiorek P., Schill R.O., Kaczmarek Ł. & Michalczyk Ł. 2016. An experimental test of eutardigrade preparation methods for light microscopy. *Zoological Journal of the Linnean Society* 178 (4): 785–793. https://doi.org/10.1111/zoj.12457

Nelson D.R., Bartels P.J. & Guil N. 2019. Tardigrade ecology. *In*: Schill R.O. (ed.) *Water Bears: The Biology of Tardigrades*: 163–210. https://doi.org/10.1007/978-3-319-95702-9_7

Nelson D.R., Adkins Fletcher R., Guidetti R., Roszkowska M., Grobys D. & Kaczmarek Ł. 2020. Two new species of Tardigrada from moss cushions (*Grimmia* sp.) in a xerothermic habitat in northeast Tennessee (USA, North America), with the first identification of males in the genus *Viridiscus*. *PeerJ* 8: e10251. https://doi.org/10.7717/peerj.10251

Nguyen L.-T., Schmidt H.A., von Haeseler A. & Minh B.Q. 2015. IQ- TREE: a fast and effective stochastic algorithm for estimating maximum likelihood phylogenies. *Molecular Biology and Evolution* 32: 268–274. https://doi.org/10.1093/molbev/msu300

Nowak B. & Stec D. 2018. An integrative description of *Macrobiotus hannae* sp. nov. (Tardigrada: Eutardigrada: Macrobiotidae: *hufelandi* group) from Poland. *Turkish Journal of Zoology* 42: 269–286. https://doi.org/10.3906/zoo-1712-31

Pilato G. 1981. Analisi di nuovi caratteri nello studio degli Eutardigradi. *Animalia* 8: 51–57.

Pilato G. & Binda M.G. 1983. Descrizione du una nuova specie di Eutardigrado d'Australia *Macrobiotus joannae* n. sp. *Animalia* 10: 262–272.

Pilato G. & Binda M.G. 2010. Definition of families, subfamilies, genera and subgenera of the Eutardigrada, and keys to their identification. *Zootaxa* 2404: 1–52. https://doi.org/10.11646/zootaxa.2404.1.1

Pilato G., Binda M.G. & Azzaro M. 1990. Tardigradi di Terra del Fuoco e Magallanes. III. *Macrobiotus punctillus*, nuova specie di Macrobiotidae del gruppo *hufelandi*. *Animalia* 17: 123–129.

Pogwizd J. & Stec D. 2022. An integrative description of a new *Richtersius* species from Greece (Tardigrada: Eutardigrada: Richtersiusidae). *Acta Zoologica Academiae Scientiarum Hungaricae* 68 (1): 1–21. https://doi.org/10.17109/AZH.68.1.1.2022

Rambaut A., Suchard M.A., Xie D. & Drummond A.J. 2014. Tracer v.1.6. Available from https://beast.bio.ed.ac.uk/Tracer [accessed 10 Sep. 2018].

Ronquist F. & Huelsenbeck J.P. 2003. MrBayes 3: Bayesian phylogenetic inference under mixed models. *Bioinformatics* 19: 1572–1574. https://doi.org/10.1093/bioinformatics/btg180

Roszkowska M., Ostrowska M., Stec D., Janko K. & Kaczmarek Ł. 2017. *Macrobiotus polypiformis* sp. nov., a new tardigrade (Macrobiotidae; *hufelandi* group) from the Ecuadorian Pacific coast, with remarks on the claw abnormalities in eutardigrades. *European Journal of Taxonomy* 327: 1–19. https://doi.org/10.5852/ejt.2017.327

Roszkowska M., Stec D., Gawlak M. & Kaczmarek Ł. 2018. An integrative description of a new tardigrade species *Mesobiotus romani* sp. nov. (Macrobiotidae: *harmsworthi* group) from the Ecuadorian Pacific coast. *Zootaxa* 4450 (5): 550–564. https://doi.org/10.11646/zootaxa.4450.5.2

Short K.A., Sands C.J., McInnes S.J., Pisani D., Stevens M.I. & Convey. P. 2022. An ancient, Antarctic-specific species complex: large divergences between multiple Antarctic lineages of the tardigrade genus *Mesobiotus*. *Molecular Phylogenetics and Evolution* 170: 107429. https://doi.org/10.1016/j.ympev.2022.107429

Stec D. 2019. *Mesobiotus datanlanicus* sp. nov., a new tardigrade species (Macrobiotidae: Mesobiotus *harmsworthi* group) from Lâm Đồng Province in Vietnam. *Zootaxa* 4679 (1): 164–180. https://doi.org/10.11646/zootaxa.4679.1.10

Stec D. 2021. Integrative descriptions of two new *Mesobiotus* species (Tardigrada, Eutardigrada, Macrobiotidae) from Vietnam. *Diversity* 13: 605. https://doi.org/10.3390/d13110605

Stec D. 2022a. An integrative description of two new *Mesobiotus* Species (Tardigrada: Eutardigrada: Macrobiotidae) with updated genus phylogeny. *Zoological Studies* 61: 85. https://doi.org/10.6620/zs.2022.61-85

Stec D. 2022b. *Macrobiotus rebecchii* sp. nov.: a new limno-terrestrial and hermaphroditic tardigrade from Kyrgyzstan. *Animals* 12 (21): 2906. https://doi.org/10.3390/ani12212906

Stec D. & Kristensen R.M. 2017. An integrative description of *Mesobiotus ethiopicus* sp. nov. (Tardigrada: Eutardigrada: Parachela: Macrobiotidae: *harmsworthi* group) from the Northern Afrotropic region. *Turkish Journal of Zoology* 41: 800–811. https://doi.org/10.3906/zoo-1701-47

Stec D., Smolak R., Kaczmarek Ł. & Michalczyk Ł. 2015. An integrative description of *Macrobiotus paulinae* sp. nov. (Tardigrada: Eutardigrada: Macrobiotidae: *hufelandi* group) from Kenya. *Zootaxa* 4052 (5): 501–526. https://doi.org/10.11646/zootaxa.4052.5.1

Stec D., Gąsiorek P., Morek W., Kosztyła P., Zawierucha K., Michno K., Kaczmarek Ł., Prokop Z.M. & Michalczyk Ł. 2016a. Estimating optimal sample size for tardigrade morphometry. *Zoological Journal of the Linnean Society* 178 (4): 776–784. https://doi.org/10.1111/zoj.12404

Stec D., Morek W., Gąsiorek P., Kaczmarek Ł. & Michalczyk Ł. 2016b. Determinants and taxonomic consequences of extreme egg shell variability in *Ramazzottius subanomalus* (Biserov, 1985) (Tardigrada). *Zootaxa* 4208 (2): 176–188. https://doi.org/10.11646/zootaxa.4208.2.5

Stec D., Zawierucha K. & Michalczyk Ł. 2017a. An integrative description of *Ramazzottius subanomalus* (Biserov, 1985) (Tardigrada) from Poland. *Zootaxa* 4300(3): 403–420. https://doi.org/10.11646/zootaxa.4300.3.4

Stec D., Morek W., Gąsiorek P., Blagden B. & Michalczyk Ł. 2017b. Description of *Macrobiotus scoticus* sp. nov. (Tardigrada: Macrobiotidae: *hufelandi* group) from Scotland by means of integrative taxonomy. *Annales Zoologici* 67 (2): 181–197. https://doi.org/10.3161/00034541ANZ2017.67.2.001

Stec D., Morek W., Gąsiorek P. & Michalczyk Ł. 2018a. Unmasking hidden species diversity within the *Ramazzottius oberhaeuseri* complex, with an integrative redescription of the nominal species for the family Ramazzottiidae (Tardigrada: Eutardigrada: Parachela). *Systematics and Biodiversity* 16 (4): 357–376. https://doi.org/10.1080/14772000.2018.1424267

Stec D., Krzywański Ł. & Michalczyk Ł. 2018b. Integrative description of *Macrobiotus canaricus* sp. nov. with notes on *M. recens* (Eutardigrada: Macrobiotidae). *European Journal of Taxonomy* 452: 1–36. https://doi.org/10.5852/ejt.2018.452

Stec D., Kristensen R.M. & Michalczyk Ł. 2018c. Integrative taxonomy identifies *Macrobiotus papei*, a new tardigrade species of the *Macrobiotus hufelandi* complex (Eutardigrada: Macrobiotidae) from the Udzungwa Mountains National Park (Tanzania). *Zootaxa* 4446 (2): 273–291. https://doi.org/10.11646/zootaxa.4446.2.7

Stec D., Arakawa K. & Michalczyk Ł. 2018d. An integrative description of *Macrobiotus shonaicus* sp. nov. (Tardigrada: Macrobiotidae) from Japan with notes on its phylogenetic position within the *hufelandi* group. *PLoS ONE* 13 (2): e0192210. https://doi.org/10.1371/journal.pone.0192210

Stec D., Roszkowska M., Kaczmarek Ł. & Michalczyk Ł. 2018e. An integrative description of a population of *Mesobiotus radiatus* (Pilato, Binda and Catanzaro, 1991) from Kenya. *Turkish Journal of Zoology* 42: 523–540. https://doi.org/10.3906/zoo-1802-43

Stec D., Kristensen R.M. & Michalczyk Ł. 2020a. An integrative description of *Minibiotus ioculator* sp. nov. from the Republic of South Africa with notes on *Minibiotus pentannulatus* Londoño *et al.*, 2017 (Tardigrada: Macrobiotidae). *Zoologischer Anzeiger* 286: 117–134. https://doi.org/10.1016/j.jcz.2020.03.007

Stec D., Krzywański Ł., Arakawa K. & Michalczyk Ł. 2020b. A new redescription of *Richtersius coronifer*, supported by transcriptome, provides resources for describing concealed species diversity within the monotypic genus *Richtersius* (Eutardigrada). *Zoological Letters* 6: 2. https://doi.org/10.1186/s40851-020-0154-y

Stec D., Dudziak M. & Michalczyk Ł. 2020c. Integrative descriptions of two new Macrobiotidae species (Tardigrada: Eutardigrada: Macrobiotoidea) from French Guiana and Malaysian Borneo. *Zoological Studies* 59: 23. https://doi.org/10.6620/ZS.2020.59-23

Stec D., Tumanov D.T. & Kristensen R.M. 2020d. Integrative taxonomy identifies two new tardigrade species (Eutardigrada: Macrobiotidae) from Greenland. *European Journal of Taxonomy* 614: 1–40. https://doi.org/10.5852/ejt.2020.614

Stec D., Krzywański Ł., Zawierucha K. & Michalczyk Ł. 2020e. Untangling systematics of the *Paramacrobiotus areolatus* species complex by an integrative redescription of the nominal species for the group, with multilocus phylogeny and species delineation within the genus *Paramacrobiotus*. *Zoological Journal of the Linnean Society* 188 (3): 694–716. https://doi.org/10.1093/zoolinnean/zlz163

Stec D., Vecchi M., Calhim S. & Michalczyk Ł. 2021a. New multilocus phylogeny reorganises the family Macrobiotidae (Eutardigrada) and unveils complex morphological evolution of the *Macrobiotus hufelandi* group. *Molecular Phylogenetics & Evolution* 160: 106987. https://doi.org/10.1016/j.ympev.2020.106987

Stec D., Vecchi M., Dudziak M., Bartels P.J., Calhim S. & Michalczyk Ł. 2021b. Integrative taxonomy resolves species identities within the *Macrobiotus pallarii* complex (Eutardigrada: Macrobiotidae). *Zoological Letters* 7: 9. https://doi.org/10.1186/s40851-021-00176-w

Stec D., Vončina K., Kristensen R.M. & Michalczyk Ł. 2022. The *Macrobiotus ariekammensis* species complex provides evidence for parallel evolution of claw elongation in macrobiotid tardigrades. *Zoological Journal of the Linnean Society* 195: 1067–1099. https://doi.org/10.1093/zoolinnean/zlab101

Surmacz B., Morek W. & Michalczyk Ł. 2019. What if multiple claw configurations are present in a sample: a case study with the description of *Milnesium pseudotardigradum* sp. nov. with unique developmental variability. *Zoological Studies* 58: 32. https://doi.org/10.6620/ZS.2019.58-32

Surmacz B., Morek W. & Michalczyk Ł. 2020. What to do when ontogenetic tracking is unavailable: a morphometric method to classify instars in *Milnesium* (Tardigrada). *Zoological Journal of the Linnean Society* 188 (3): 797–808. https://doi.org/10.1093/zoolinnean/zlz099

Tamura K., Stecher G. & Kumar S. 2021. MEGA11: Molecular Evolutionary Genetics Analysis Version 11. *Molecular Biology and Evolution* 38 (7): 3022–3027. https://doi.org/10.1093/molbev/msab120

Trifinopoulos J., Nguyen L.-T., von Haeseler A. & Minh B.Q. 2016. W-IQ-TREE: a fast online phylogenetic tool for maximum likelihood analysis. *Nucleic Acids Research* 44: 232–235. https://doi.org/10.1093/nar/gkw256

Tumanov D.V. 2020. Integrative description of *Mesobiotus anastasiae* sp. nov. (Eutardigrada, Macrobiotoidea) and first record of *Lobohalacarus* (Chelicerata, Trombidiformes) from the Republic of South Africa. *European Journal of Taxonomy* 726 (1): 102–131. https://doi.org/10.5852/ejt.2020.726.1179

Vaidya G., Lohman D.J. & Meier R. 2011. SequenceMatrix: concatenation software for the fast assembly of multi-gene datasets with character set and codon information. *Cladistics* 27: 171–180. https://doi.org/10.1111/j.1096-0031.2010.00329.x

Vecchi M. & Stec D. 2021. Integrative descriptions of two new *Macrobiotus* species (Tardigrada, Eutardigrada, Macrobiotidae) from Mississippi (USA) and Crete (Greece). *Zoosystematics and Evolution* 97 (1): 281–306. https://doi.org/10.3897/zse.97.65280

Vecchi M., Cesari M., Bertolani R., Jönsson K.I., Rebecchi L. & Guidetti R. 2016. Integrative systematic studies on tardigrades from Antarctica identify new genera and new species within Macrobiotoidea and Echiniscoidea. *Invertebrate Systematics* 30 (4): 303–322. https://doi.org/10.1071/IS15033

Vecchi M., Stec D., Tommi V., Ryndov S., Chartrain J. & Calhim S. 2022a. *Macrobiotus naginae* sp. nov., a new xerophilous tardigrade species from Rokua sand dunes (Finland). *Zoological Studies* 61: 22. https://doi.org/10.6620/ZS.2022.61-22

Vecchi M., Choong H. & Calhim S. 2022b. *Sisubiotus hakaiensis* sp. nov. (Tardigrada, Macrobiotidae), a new tardigrade species from Calvert Island (British Columbia, Canada). *European Journal of Taxonomy* 823: 64–81. https://doi.org/10.5852/ejt.2022.823.1815

Vincenzi J., Cesari M., Kaczmarek Ł., Roszkowska M., Mioduchowska M., Rebecchi L., Kiosya Y. & Guidetti R. 2023. The xerophilic genera *Xerobiotus* and *Pseudohexapodibius* (Macrobiotidae; Tardigrada): biodiversity, biogeography and phylogeny. *Zoological Journal of the Linnean Society* 200 (1): 111–141. https://doi.org/10.1093/zoolinnean/zlad129

Vinarski M.V. 2020. Roots of the taxonomic impediment: Is the "integrativeness" a remedy? *Integrative Zoology* 15: 2–15. https://doi.org/10.1111/1749-4877.12393

Yuan Z., Wang Y., Liu Q., Liu L. & Li X.-C. 2022. *Macrobiotus hupingensis*, a new tardigrade species in the *Macrobiotus pallarii* complex from China. *Zoological Studies* 61: 86. https://doi.org/10.6620/ZS.2022.61-86

Manuscript received: 16 September 2023
Manuscript accepted: 14 November 2023
Published on 29 March 2024
Topic editor: Magalie Castelin
Section editor: Fabio Stoch
Desk editor: Natacha Beau

Supplementary files

Supp. file 1. Raw morphometric data underling the description of *Macrobiotus ovovittatus* sp. nov.
https://doi.org/10.5852/ejt.2024.930.2481.11047

Supp. file 2. Raw morphometric data underling the description of *Macrobiotus mileri* sp. nov.
https://doi.org/10.5852/ejt.2024.930.2481.11049

Supp. file 3. Model selections of sequence evolution for BI and ML analyses and raw trees.
https://doi.org/10.5852/ejt.2024.930.2481.11051

Supp. file 4. Outputs from the ASAP analyses.
https://doi.org/10.5852/ejt.2024.930.2481.11055

Appendix 1 (continued on next 5 pages)**.** Sequences used for phylogenetic analysis. Bold font indicates sequences obtained in this study.

Species	18S	28S	ITS-2	COI	Source
Macrobiotus ovovittatus GL.001.01	**OR543310**	**OR543318**	**OR543314**	**OR544395**	**this study**
Macrobiotus ovovittatus GL.001.02	**OR543311**	**OR543319**	**OR543315**	**OR544396**	**this study**
Macrobiotus mileri IL.001.01 (forma porata)	**OR543312**	**OR543320**	**OR543316**	**OR544397**	**this study**
Macrobiotus mileri IL.001.02 (forma aporata)	**OR543313**	**OR543321**	**OR543317**	**OR544398**	**this study**
Macrobiotus mileri IL.001.03 (forma porata)				**OR544399**	**this study**
Macrobiotus mileri IL.001.04 (forma aporata)				**OR544400**	**this study**
Macrobiotus kosmali M8.1	OP142472	OP143765	OP153786	OP141639	Kayastha *et al.* (2023)
Macrobiotus kosmali M8.2	OP142473	OP143766		OP141640	Kayastha *et al.* (2023)
Macrobiotus hupingensis	MW183923	MZ470349	MZ474842	MW186952	Yuan *et al.* (2022)
Macrobiotus dolosus C3209_2	OP596290			OP561772	Bertolani *et al.* (2023)
Macrobiotus dolosus C3209_US2				OP561773	Bertolani *et al.* (2023)
Macrobiotus dolosus C3209_4				OP561774	Bertolani *et al.* (2023)
Macrobiotus dolosus C3581_V6	OP596292			OP561775	Bertolani *et al.* (2023)
Macrobiotus dolosus C3209_1	OP596289				Bertolani *et al.* (2023)
Macrobiotus dolosus C3581_V5	OP596291				Bertolani *et al.* (2023)
Macrobiotus siderophilus C2796_2	OP596293			OP561776	Bertolani *et al.* (2023)
Macrobiotus siderophilus C3282_UFK				OP561777	Bertolani *et al.* (2023)
Macrobiotus siderophilus C3282_UFL				OP561778	Bertolani *et al.* (2023)
Macrobiotus siderophilus C3282_UFM				OP561779	Bertolani *et al.* (2023)
Macrobiotus siderophilus C3282_UFN	OP596294			OP561780	Bertolani *et al.* (2023)
Macrobiotus siderophilus C3282_UFO				OP561781	Bertolani *et al.* (2023)
Macrobiotus siderophilus C3282_UFP				OP561782	Bertolani *et al.* (2023)
Macrobiotus fonturai C2861_5	OP596295			OP561783	Bertolani *et al.* (2023)
Macrobiotus fonturai C2861_US1	OP596296			OP561784	Bertolani *et al.* (2023)
Macrobiotus muralis C2861_FG	OP596297				Bertolani *et al.* (2023)
Macrobiotus muralis C2861_6	OP596298				Bertolani *et al.* (2023)
Macrobiotus cf. *muralis* C3251_2	OP596299			OP561785	Bertolani *et al.* (2023)

Appendix 1. Sequences used for phylogenetic analysis. Bold font indicates sequences obtained in this study.

Species	18S	28S	ITS-2	COI	Source
Macrobiotus cf. *muralis* C3251_3	OP596300			OP561786	Bertolani *et al.* (2023)
Macrobiotus cf. *muralis* C3251_FA	OP596301			OP561787	Bertolani *et al.* (2023)
Macrobiotus cf. *muralis* C3251_4				OP561788	Bertolani *et al.* (2023)
Macrobiotus cf. *muralis* C3251_5				OP561789	Bertolani *et al.* (2023)
Macrobiotus hufelandi C2953_A02	OP596302			HQ876586	Bertolani *et al.* (2023), Bertolani *et al.* (2011)
Macrobiotus cf. *hufelandi* C2959_A01	OP596303			HQ876590	Bertolani *et al.* (2023), Bertolani *et al.* (2011)
Macrobiotus cf. *hufelandi* C2959_A02	OP596304			HQ876591	Bertolani *et al.* (2023), Bertolani *et al.* (2011)
Macrobiotus vladimiri C2688_A02	OP596305			HM136932	Bertolani *et al.* (2023), Bertolani *et al.* (2011)
Macrobiotus terminalis C2868_N02	OP596308			JN673959	Bertolani *et al.* (2023), Bertolani *et al.* (2011)
Macrobiotus cf. *nelsonae* 1	HQ604965				Bertolani *et al.* (2014)
Macrobiotus cf. *nelsonae* 2	HQ604966				Bertolani *et al.* (2014)
Macrobiotus rebecchii 1	OP479887			OP477442	Stec (2022b)
Macrobiotus rebecchii 2	OP479888			OP477443	Stec (2022b)
Macrobiotus kyoukenus v3	ON818312		ON818300	ON809461	Cesari *et al.* (2022)
Macrobiotus kyoukenus us3	ON818314		ON818301	ON809462	Cesari *et al.* (2022)
Macrobiotus kyoukenus us4	ON818315		ON818302	ON809463	Cesari *et al.* (2022)
Macrobiotus kyoukenus us5	ON818316		ON818303	ON809464	Cesari *et al.* (2022)
Macrobiotus scoticus DK 1	OK663218	OK663228	OK663207	OK662989	Vecchi *et al.* (2022a)
Macrobiotus scoticus DK 2	OK663217	OK663229	OK663206	OK662988	Vecchi *et al.* (2022a)
Macrobiotus naginae S226_1	OK663219	OK663230	OK663209	OK662990	Vecchi *et al.* (2022a)
Macrobiotus naginae S226_2	OK663220	OK663231	OK663208	OK662991	Vecchi *et al.* (2022a)
Macrobiotus naginae S605_1	OK663221	OK663232	OK663210	OK662992	Vecchi *et al.* (2022a)
Macrobiotus naginae S605_2	OK663222	OK663233	OK663211	OK662993	Vecchi *et al.* (2022a)
Macrobiotus sandrae S859_1	OK663223	OK663234	OK663212	OK662994	Vecchi *et al.* (2022a)
Macrobiotus cf. *sapiens*	OK663226	OK663237	OK663215	OK662997	Vecchi *et al.* (2022a)
Macrobiotus sandrae 1	MW695445			HQ876573	Bertolani *et al.* (2011); Ben Marnissi *et al.* (2021)
Macrobiotus sandrae 2	MW695446			HQ876577	Bertolani *et al.* (2011); Ben Marnissi *et al.* (2021)
Macrobiotus azzunae 1	MW695447		MW695454	MW698697	Ben Marnissi *et al.* (2021)
Macrobiotus azzunae 2	MW695448		MW695455	MW698698	Ben Marnissi *et al.* (2021)

Appendix 1. Sequences used for phylogenetic analysis. Bold font indicates sequences obtained in this study.

Species	18S	28S	ITS-2	COI	Source
Macrobiotus birendrai	MW680641	MW680644	MW680418	MW656266	Kayastha *et al.* (2021)
Macrobiotus a. groenlandicus 1	MZ463664	MZ463679	MZ463654	MZ461006	Stec *et al.* (2022)
Macrobiotus a. groenlandicus 2	MZ463663	MZ463678	MZ463655	MZ461007	Stec *et al.* (2022)
Macrobiotus a. groenlandicus 3	MZ463662	MZ463677	MZ463653	MZ461005	Stec *et al.* (2022)
Macrobiotus kirghizicus 1	MZ463666	MZ463672	MZ463659	MZ461002	Stec *et al.* (2022)
Macrobiotus kirghizicus 2	MZ463665	MZ463671	MZ463660	MZ461003	Stec *et al.* (2022)
Macrobiotus kirghizicus 3	MZ463667	MZ463673	MZ463661	MZ461004	Stec *et al.* (2022)
Macrobiotus a. ariekammensis 1	MZ463668	MZ463674	MZ463656	MZ460999	Stec *et al.* (2022)
Macrobiotus a. ariekammensis 2	MZ463669	MZ463675	MZ463657	MZ461000	Stec *et al.* (2022)
Macrobiotus a. ariekammensis 3	MZ463670	MZ463676	MZ463658	MZ461001	Stec *et al.* (2022)
Macrobiotus aff. *pseudohufelandi* PL	MN888373	MN888358	MN888345	MN888325	Stec *et al.* (2021a)
Macrobiotus aff. *pseudohufelandi* ZA	MN888374	MN888359	MN888345	MN888326	Stec *et al.* (2021a)
Macrobiotus annewintersae 1	MW588024	MW588030	MW588019	MW593927	Vecchi & Stec (2021)
Macrobiotus annewintersae 2	MW588025	MW588031	MW588018	MW593928	Vecchi & Stec (2021)
Macrobiotus basiatus	MT498094	MT488397	MT505165	MT502116	Nelson *et al.* (2020)
Macrobiotus caelestis	MK737073	MK737071	MK737072	MK737922	Coughlan *et al.* (2019)
Macrobiotus canaricus 1	MH063925	MH063934	MH063928	MH057765	Stec *et al.* (2018b)
Macrobiotus canaricus 2			MH063929	MH057766	Stec *et al.* (2018b)
Macrobiotus cf. *polonicus* 1	MW588026	MW588032	MW588021	MW593929	Vecchi & Stec (2021)
Macrobiotus cf. *polonicus* 2	MW588027	MW588033	MW588020	MW593930	Vecchi & Stec (2021)
Macrobiotus cf. *recens* 1	MH063927	MH063936	MH063932	MH057768	Stec *et al.* (2018b)
Macrobiotus cf. *recens* 2			MH063933	MH057769	Stec *et al.* (2018b)
Macrobiotus crustulus	MT261912	MT261903	MT261907	MT260371	Stec *et al.* (2020c)
Macrobiotus engbergi 1	MN443039	MN443034	MN443036	MN444824	Stec *et al.* (2020d)
Macrobiotus engbergi 2			MN443037	MN444825	Stec *et al.* (2020d)
Macrobiotus engbergi 3				MN444826	Stec *et al.* (2020d)
Macrobiotus glebkai	MW247177	MW247176	MW247180	MW246134	Kiosya *et al.* (2021)
Macrobiotus hannae	MH063922	MH063924	MH063923	MH057764	Nowak & Stec (2018)
Macrobiotus kamilae 1	MK737070	MK737064	MK737067	MK737920	Coughlan & Stec (2019)
Macrobiotus kamilae 2				MK737921	Coughlan & Stec (2019)
Macrobiotus kristenseni	KC193577			KC193573	Guidetti *et al.* (2013)
Macrobiotus macrocalix	MH063926	MH063935	MH063931	MH057767	Stec *et al.* (2018b)
Macrobiotus noongaris 1	MK737069	MK737063	MK737065	MK737919	Coughlan & Stec (2019)

Appendix 1. Sequences used for phylogenetic analysis. Bold font indicates sequences obtained in this study.

Species	18S	28S	ITS-2	COI	Source
Macrobiotus noongaris 2			MK737066		Coughlan & Stec (2019)
Macrobiotus papei	MH063881	MH063880	MH063921	MH057763	Stec *et al.* (2018c)
Macrobiotus paulinae	KT935502	KT935501	KT935500	KT951668	Stec *et al.* (2015)
Macrobiotus polonicus AT 1	MN888369	MN888355	MN888337	MN888317	Stec *et al.* (2021a)
Macrobiotus polonicus AT 2			MN888338	MN888318	Stec *et al.* (2021a)
Macrobiotus polonicus AT 3				MN888319	Stec *et al.* (2021a)
Macrobiotus polonicus SK 1	MN888370	MN888356	MN888332	MN888320	Stec *et al.* (2021a)
Macrobiotus polonicus SK 2			MN888333	MN888321	Stec *et al.* (2021a)
Macrobiotus polonicus SK 3			MN888334		Stec *et al.* (2021a)
Macrobiotus porifini 1	MT241900	MT241897		MT246659	Kuzdrowska *et al.* (2021)
Macrobiotus porifini 2		MT241898		MT246660	Kuzdrowska *et al.* (2021)
Macrobiotus porifini 3		MT241899		MT246661	Kuzdrowska *et al.* (2021)
Macrobiotus polypiformis 1	KX810008	KX810009	KX810010	KX810011	Roszkowska *et al.* (2017)
Macrobiotus polypiformis 2				KX810012	Roszkowska *et al.* (2017)
Macrobiotus pseudohufelandi 1	HQ604989			AY598776	Bertolani *et al.* (2014)
Macrobiotus pseudohufelandi 2	HQ604990			AY598777	Bertolani *et al.* (2014)
Macrobiotus rybaki 1	MW588029	MW588034	MW588022	MW593931	Vecchi & Stec (2021)
Macrobiotus rybaki 2	MW588028	MW588035	MW588023	MW593932	Vecchi & Stec (2021)
Macrobiotus scoticus	KY797265	KY797266	KY797268	KY797267	Stec *et al.* (2017b)
Macrobiotus shonaicus 1	MG757132	MG757133	MG757134	MG757136	Stec *et al.* (2018d)
Macrobiotus shonaicus 2			MG757135	MG757137	Stec *et al.* (2018d)
Macrobiotus sottilei	MW247178	MW247175	MW247179	MW246133	Kiosya *et al.* (2021)
Macrobiotus vladimiri FI	MN888375	MN888360	MN888347	MN888327	Stec *et al.* (2021a)
Macrobiotus wandae	MN435112	MN435116	MN435120	MN482684	Kayastha *et al.* (2020b)
Macrobiotus pallarii 1	MT809069	MT809081	MT809094	MT807924	Stec *et al.* (2021b)
Macrobiotus pallarii 2	MT809070	MT809082	MT809095	MT807925	Stec *et al.* (2021b)
Macrobiotus pallarii 3	MT809071	MT809083	MT809096	MT807926	Stec *et al.* (2021b)
Macrobiotus pseudopallarii 1	MT809067	MT809079	MT809091	MT807921	Stec *et al.* (2021b)
Macrobiotus pseudopallarii 2	MT809068	MT809080	MT809092	MT807922	Stec *et al.* (2021b)
Macrobiotus ripperi FI	MT809076	MT809089	MT809103	MT807930	Stec *et al.* (2021b)
Macrobiotus ripperi PL	MT809074	MT809086	MT809100	MT807933	Stec *et al.* (2021b)
Macrobiotus margoae US	MT809072	MT809084	MT809098	MT807927	Stec *et al.* (2021b)
Macrobiotus gretae 1	MW588434		MW588431	MW581665	Massa *et al.* (2021)
Macrobiotus gretae 2	MW588437		MW588433	MW581668	Massa *et al.* (2021)

Appendix 1. Sequences used for phylogenetic analysis. Bold font indicates sequences obtained in this study.

Species	18S	28S	ITS-2	COI	Source
Macrobiotus gretae 3	MW588435		MW588432	MW581666	Massa *et al.* (2021)
Macrobiotus gretae 4	MW588436			MW581667	Massa *et al.* (2021)
Sisubiotus hakaiensis 1	OM523054	OM523059	OM523057	OM523181	Vecchi *et al.* (2022b)
Sisubiotus hakaiensis 2	OM523055	OM523060	OM523058	OM523182	Vecchi *et al.* (2022b)
Sisubiotus spectabilis FI 1	MN888371	MN888357	MN888331	MN888322	Stec *et al.* (2021a)
Sisubiotus spectabilis FI 2				MN888323	Stec *et al.* (2021a)
Sisubiotus spectabilis NO	MN888372	MN888364	MN888344	MN888324	Stec *et al.* (2021a)
Mesobiotus anastasiae	MT903468	MT903612	MT903470	MT904513	Tumanov (2020)
Mesobiotus hilariae	KT226070			KT226108	Vecchi *et al.* (2016)
Mesobiotus cf. *barabanovi*	MN310392	MN310388	MN310390	MN313170	Kaczmarek *et al.* (2020)
Mesobiotus datanlanicus	MK584659	MK584658	MK584657	MK578905	Stec (2019)
Mesobiotus dilimanensis	MN257048	MN257049	MN257050	MN257047	Itang *et al.* (2020)
Mesobiotus ethiopicus	MF678793	MF678792	MN122776	MF678794	Stec & Kristensen (2017)
Mesobiotus fiedleri	MH681585	MH681693	MH681724	MH676056	Kaczmarek *et al.* (2020)
Mesobiotus harmsworthi	MH197146	MH197264	MH197154	MH195150	Kaczmarek *et al.* (2018)
Mesobiotus insanis	MF441488	MF441489	MF441490	MF441491	Mapalo *et al.*(2017)
Mesobiotus occultatus	MH197147		MH197155	MH195152	Kaczmarek *et al.* (2018)
Mesobiotus philippinicus	KX129793	KX129794	KX129795	KX129796	Mapalo *et al.* (2016)
Mesobiotus radiatus 1	MH197153	MH197152	MH197267	MH195147	Stec *et al.* (2018e)
Mesobiotus radiatus 2			MH197268	MH195148	Stec *et al.* (2018e)
Mesobiotus romani	MH197158	MH197151	MH197150	MH195149	Roszkowska *et al.* (2018)
Mesobiotus imperialis 1	OL257854	OL257866		OL311514	Stec (2021)
Mesobiotus imperialis 2	OL257855	OL257867		OL311515	Stec (2021)
Mesobiotus marmoreus 1	OL257856	OL257868	OL257861	OL311516	Stec (2021)
Mesobiotus marmoreus 2	OL257857	OL257869	OL257862	OL311517	Stec (2021)
Mesobiotus marmoreus 3	OL257858	OL257870	OL257863	OL311518	Stec (2021)
Mesobiotus skoracki		MW680636		MW656257	Kayastha *et al.* (2021)
Mesobiotus sp. Macro07_042	MW751942			MW727957	Short *et al.* (2022)
Mesobiotus cf. *furciger* Macro06_296	MW751936			MW727958	Short *et al.* (2022)
Mesobiotus cf. *furciger* Macro06_310	MW751937			MW727961	Short *et al.* (2022)
Mesobiotus cf. *furciger* Macro06_313	MW751939			MW727960	Short *et al.* (2022)
Mesobiotus cf. *furciger* CC_MF_4	MW751949			MW727933	Short *et al.* (2022)
Mesobiotus cf. *furciger* ABDC_MF_3	MW751944			MW727932	Short *et al.* (2022)
Mesobiotus cf. *furciger* KPRI_MF_1	MW751962			MW727934	Short *et al.* (2022)

Appendix 1. Sequences used for phylogenetic analysis. Bold font indicates sequences obtained in this study.

Species	18S	28S	ITS-2	COI	Source
Mesobiotus cf. *furciger* HMI_MF_1	MW751957			MW727941	Short *et al.* (2022)
Mesobiotus cf. *furciger* EBNI_MF_2	MW751952			MW727937	Short *et al.* (2022)
Mesobiotus cf. *furciger* EBNI_MF_4	MW751954			MW727938	Short *et al.* (2022)
Mesobiotus cf. *furciger* PSAI_MF_2	MW751967			MW727939	Short *et al.* (2022)
Mesobiotus cf. *furciger* Macro06_162	MW751934			MW727955	Short *et al.* (2022)
Mesobiotus cf. *furciger* Macro06_171	MW751935			MW727956	Short *et al.* (2022)
Mesobiotus cf. *furciger* JN07_MF_1	MW751959			MW727951	Short *et al.* (2022)
Mesobiotus cf. *furciger* JN07_MF_4	MW751960			MW727953	Short *et al.* (2022)
Mesobiotus cf. *furciger* JN07_MF_8	MW751961			MW727947	Short *et al.* (2022)
Mesobiotus cf. *furciger* FN01_MF_6	MW751955			MW727945	Short *et al.* (2022)
Mesobiotus diegoi 1	OP142527	OP142520	OP142514	OP143858	Stec (2022a)
Mesobiotus diegoi 2	OP142526	OP142521	OP142515	OP143857	Stec (2022a)
Mesobiotus maklowiczi 1	OP142525	OP142518		OP143855	Stec (2022a)
Mesobiotus maklowiczi 2	OP142524	OP142519		OP143856	Stec (2022a)
Mesobiotus peterseni 1	OP142528	OP142522	OP142516	OP143859	Stec (2022a)
Mesobiotus peterseni 2	OP142529	OP142523	OP142517	OP143860	Stec (2022a)
Minibiotus ioculator	MT023998	MT024041	MT024000	MT023412	Stec *et al.* (2020a)
Paramacrobiotus areolatus	MH664931	MH664948	MH666080	MH675998	Stec *et al.* (2020e)
Tenuibiotus zandrae	MN443040	MN443035	MN443038	MN444827	Stec *et al.* (2020d)